CHAPTER 3

RESULTS AND DISCUSSIONS

3.1 Cyclic voltammetry of blank solution at glassy carbon electrode

Cyclic voltammogram of CH_3CN containing 0.1 M TBAP as all blank solution was recorded in the potential range of 0.000 to -2.000 V vs Ag/AgCl. No significant peak was obtained, implying that there was no significant impurities as shown in Figure 5.

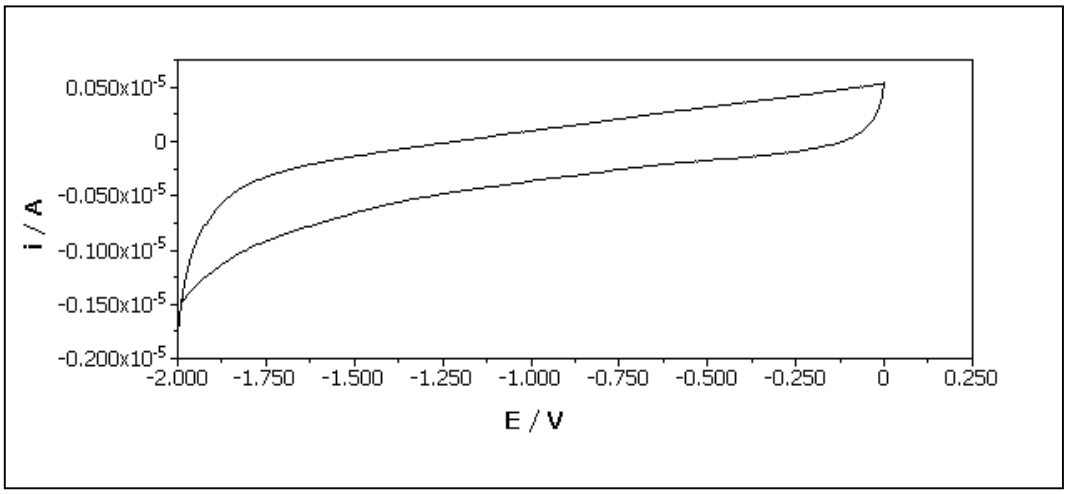

Figure 5 Cyclic voltammogram of blank solution at glassy carbon electrode in 50 mL CH_3CN containing 0.1 M TBAP with scan rate of 120 mV s^{-1}.

3.2 Electrochemical behavior of 1,4-dihydroxyanthraquinone at glassy carbon electrode

Figure 6 shows the structures of all quinone compounds was studied the electrochemical behavior. The cyclic voltammogram of 1,4-dihydroxyanthraquinone shows two redox couples in CH_3CN as in Figure 7. It undergoes two successive and distinct reduction/oxidation processes. The first reduction/oxidation appear at -0.682 V and -0.615 V vs Ag/AgCl and $Ipc_1 = 9.500 \times 10^{-6}$ A and $Ipa_1 = 1.207 \times 10^{-5}$ A respectively. This behavior shows

the second reduction at -1.151 V and Ipc_2 = 1.046 x 10^{-5} A. The second oxidation occurs at -1.082 V vs Ag/AgCl and Ipa_2 = 8.968 x 10^{-6} A. Both couples are somewhat chemically reversible (Ipa_1/Ipc_1= 1.270) and (Ipa_2/Ipc_2= 0.893). The ΔEp_1 of 1,4-dihydroxyanthraquinone (67 mV) is somewhat higher than the theoretical value (> 59 mV) which indicates that the electron transfer is quite slow at this scan rate (120 mV s^{-1}) and slow electron transfer cause the peak separation to increase of the first couple. The first reduction reaction corresponds to the transformation of 1,4-dihydroxyanthraquinone into semiquinone and the second to the transformation of semiquinone into quinone dianion.

3.3 Electrochemical behavior of anthraquinone at glassy carbon electrode

Cyclic voltammogram of anthraquinone solution was performed in the potential window from 0.000 to -2.000 vs Ag/AgCl. The cyclic voltammogram of anthraquinone displays two redox couple as shown in Figure 8. The first redox couple occurs at Epc_1 = -0.934 V with Ipc_1= 6.707 x 10^{-6} A and Epa_1 = -0.860 V with Ipa_1= 7.252 x 10^{-6} A vs Ag/AgCl. The first formal potential ($E_1^{0\prime}$) is calculated be 0.897 vs Ag/AgCl. The second reduction and oxidation peaks appears at Epc_2= -1.402 V with Ipc_2=1.938 x 10^{-6} A and Epa_2= -1.371 V with Ipa_2= 2.498 x 10^{-6} A vs Ag/AgCl respectively. The first redox couple is chemically reversible (Ipa_1/Ipc_1 = 1.081). The second couple is somewhat chemically reversible (Ipa_2/Ipc_2 = 1.288). The ΔEp_1 of anthraquinone equals to 74 mV which is somewhat higher than the theoretical value (> 59 mV) which implies that the electron transfer is quite slow at this scan rate (120 mV s^{-1}). The first reduction reaction corresponds to the transformation of anthraquinone (AQ) into semiquinone ($AQ^{\cdot}$-) and the second to the quinone dianion (AQ^{2-}).

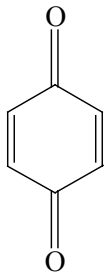

1,4-Benzoquinone

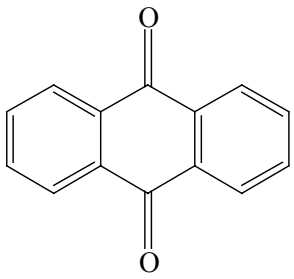

Anthraquinone

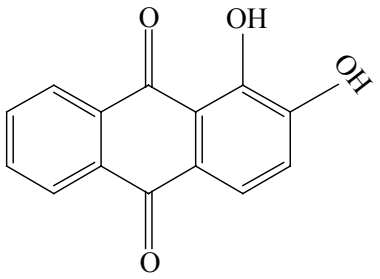

1,2-Dihydroxyanthraquinone

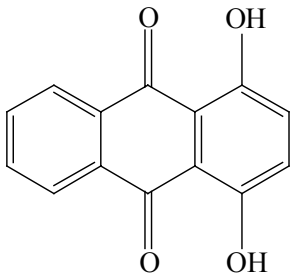

1,4-Dihydroxyanthraquinone

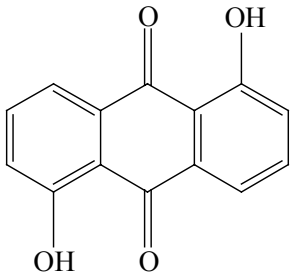

1,5-Dihydroxyanthraquinone

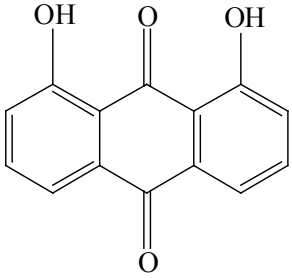

1,8-Dihydroxyanthraquinone

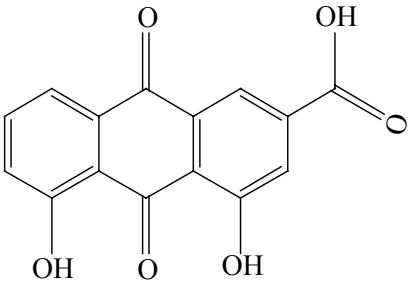

4,5-Dihydroxyanthraquinone-2-carboxylic acid

Figure 6 The structure of quinone compounds

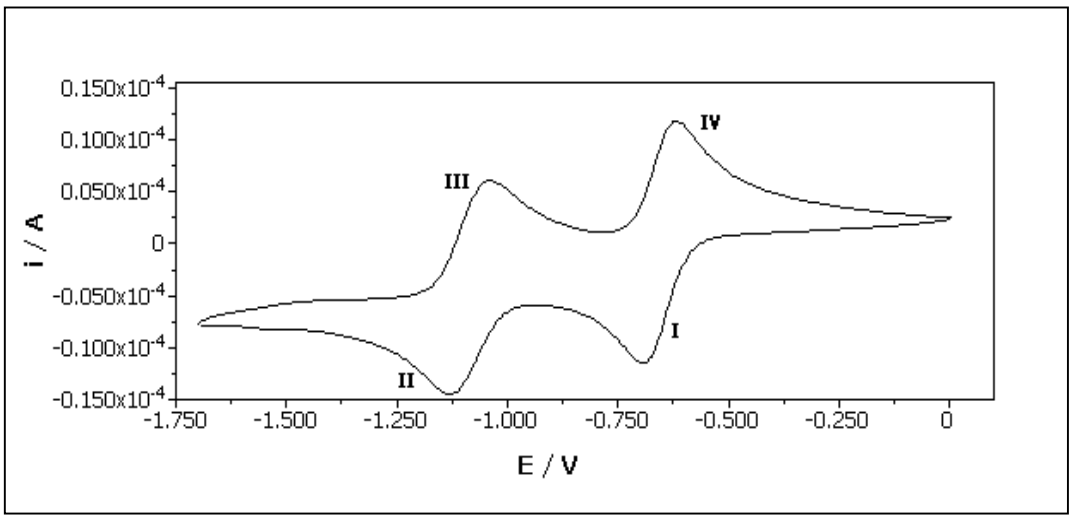

Figure 7 Cyclic voltammogram of 1.0 x 10^{-3} M 1,4-dihydroxyanthraquinone at GCE in 50 mL CH_3CN containing 0.1 M TBAP as supporting electrolyte with scan rate of 120 mV s^{-1}.

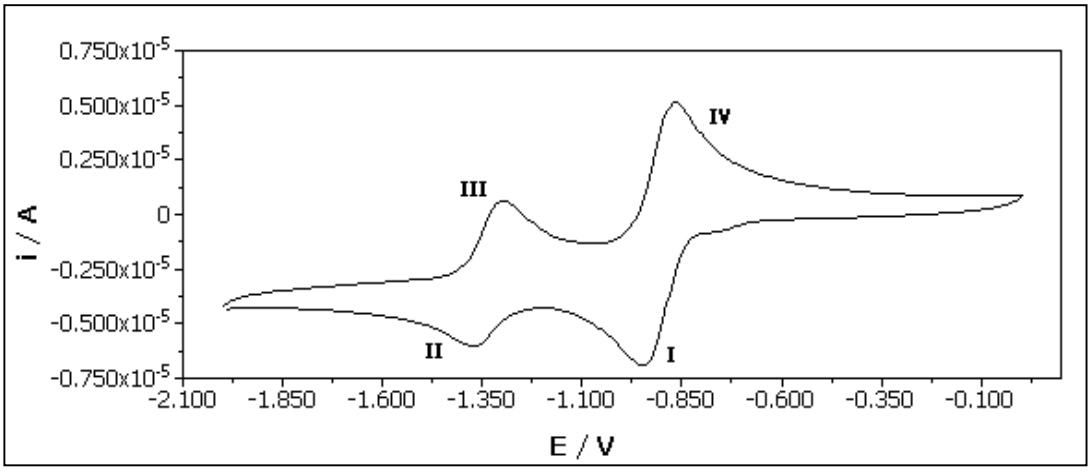

Figure 8 Cyclic voltammogram of 1.0 x 10^{-3} M anthraquinone at GCE in 50 mL CH_3CN containing 0.1 M TBAP as supporting electrolyte with scan rate of 120 mV s^{-1}.

3.4 Electrochemical behavior of 1, 2-dihydroxyanthraquinone at glassy carbon electrode

Cyclic voltammogram of blank was performed in the potential window from 0.000 to -2.000 V vs Ag/AgCl. It was found that there were no significant impurities. The electrochemical behavior of 1,2 - dihydroxyanthraquinone displays the first reduction peak at

Epc_1 = -0.751 V vs Ag/AgCl with Ipc_1= 8.331 x 10^{-6} A and the first oxidation (Epa_1) is - 0.656 V vs Ag/AgCl with Ipa_1 = 9.036 x 10^{-6} A as shown in Figure 9. The first formal potential ($E_1^{0'}$) is equal to -0.704 V vs Ag/AgCl. The second reduction peak and its corresponding oxidation peak which appears at -1.243 V with Ipc_2 = 3.272 x 10^{-6} A and -1.170 V vs Ag/AgCl with Ipa_2 = 3.793 x 10^{-6} A respectively. The first couple is chemically reversible (Ipa_1/Ipc_1 = 1.088). The second couple is somewhat chemically reversible (Ipa_2/Ipc_2 = 1.159). The ΔEp_1 of 1,2-dihydroxyanthraquinone (92 mV) is somewhat higher than the theoretical value (> 59 mv) which implies that the electron transfer is quite slow at this scan rate (l20 mV s^{-1}) and slow electron transfer causes the peak separation to increase of the first couple. The small peaks occurred with some kinds of shoulder or interference peaks which could due to the impurities in 1,2-dihydroxyanthraquinone compound (96% purity). The first reduction reaction conforms to the transformation of 1,2-dihydroxyanthraquinone into semiquinone and the second to the transformation of semiquinone in to quinone dianion.

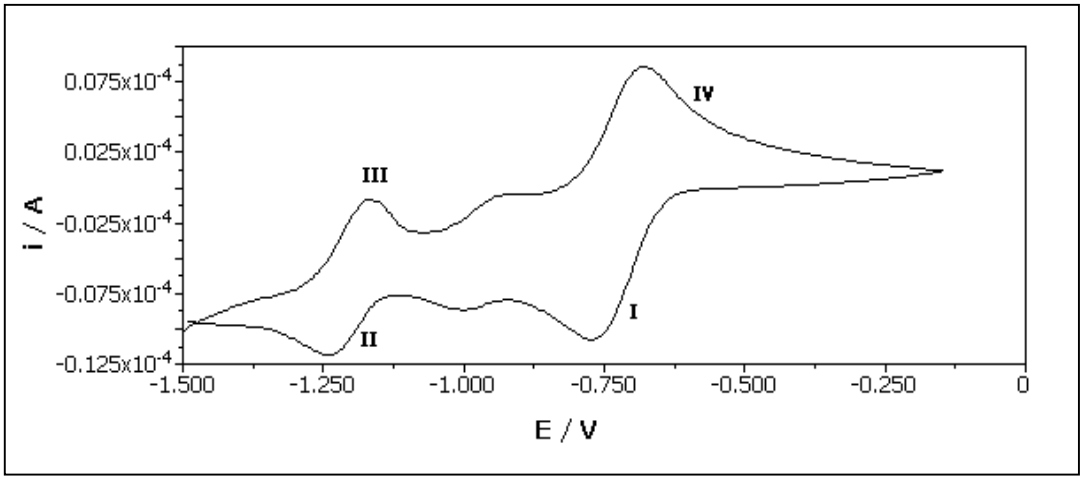

Figure 9 Cyclic voltammogram of 1.0 x 10^{-3} M 1,2-dihydroxyanthraquinone at GCE in 50 mL CH_3CN containing 0.1 M TBAP as supporting electrolyte with scan rate of 120 mV s^{-1}.

3.5 Electrochemical behavior of 1,5–dihydroxyanthraquinone at glassy carbon electrode

Cyclic voltammogram of 1,5–dihydroxyanthraquinone as shown in Figure 10 which was recorded in the potential window of 0.000 to -2.000 V vs Ag/AgCl.

1,5-dihydroxyanthraquinone exhibits two redox couples. The first redox couple occurs at Epc_1 = -0.648 V with Ipc_1 = 1.433 x 10^{-6} A and Epa_1 = -0.587 V with Ipa_1 = 1.168 x 10^{-6} A. The second redox couple occurs at Epc_2 = -0.973 V with Ipc_2 = 9.271 x 10^{-6} A and Epa_2 = -0.899 V with Ipa_2 = 8.790 x 10^{-6} A. The ΔEpc (61 mV) is rather high than the theoretical value (Ep = 59 mV), implying that the electron transfer is slow at 120 mV s^{-1} slow electron transfer cause the peak separation to increase. The first couple (I and IV) occurs at $E^{0'}_1$ = -0.618 V vs Ag/AgCl. Both couples are somewhat chemically reversible (Ipa_1/Ipc_1 = 1.227) and (Ipa_2/Ipc_2= 0.950). The first reduction reaction conforms = -0.650 to the transformation of 1,5-dihydroxyanthraquinone into semiquinone and the second to the transformation of semiquinone into quinone dianion.

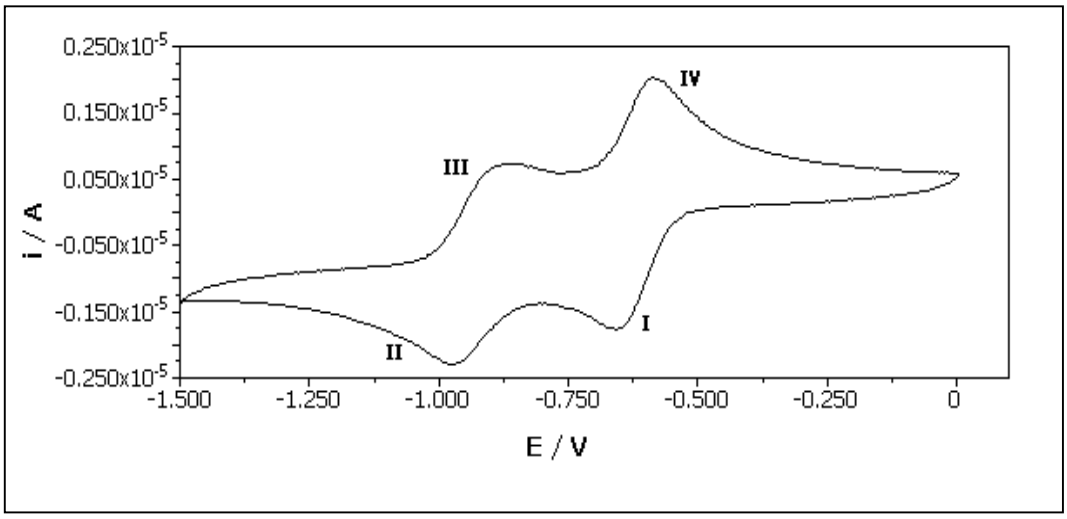

Figure 10 Cyclic voltammogram of 1.0 x 10^{-3} M 1,5-dihydroxyanthraquinone at GCE in 50 mL CH_3CN containing 0.1 M TBAP as supporting electrolyte with scan rate of 120 mV s^{-1}.

3.6 Electrochemical behavior of 1,8–dihydroxyanthraquinone at glassy carbon electrode

Cyclic voltammogram of 1,8–dihydroxyanthraquinone solution was performed in the potential range from 0.000 to -1.500 V vs Ag/AgCl. The cyclic voltammogram of 1,8–dihydroxyanthraquinone shows two redox couples in CH_3CN as in Figure 11. The first reduction/oxidation occurs at -0.656 V with Ipc_1 = 1.312 x 10^{-5} A and -0.592 V vs Ag/AgCl with

Ipa_1 = 1.232 x 10^{-5} A respectively. It also displays the second reduction at -1.151 V with Ipc_2 = 7.356 x 10^{-6} A and the second oxidation at -1.088 V with Ipa_2 = 7.743 x 10^{-6} A vs Ag/AgCl. Both couple are chemically reversible (Ipa_1/Ipc_1 = 0.939) and (Ipa_2/Ipc_2 = 1.052). The formal potential of the first couple is equal to -0.607 V vs Ag/AgCl. The ΔEp_1 of 1,8–dihydroxyanthraquinone (64 mV) is a little higher than the theoretical value (59 mV) which imply that the electron transfer is quite slow at this scan rate (120 mV s^{-1}) The first reduction reaction conforms to the transformation of 1,8–dihydroxyanthraquinone into semiquinone and the second to the change of semiquinone into quinone dianion.

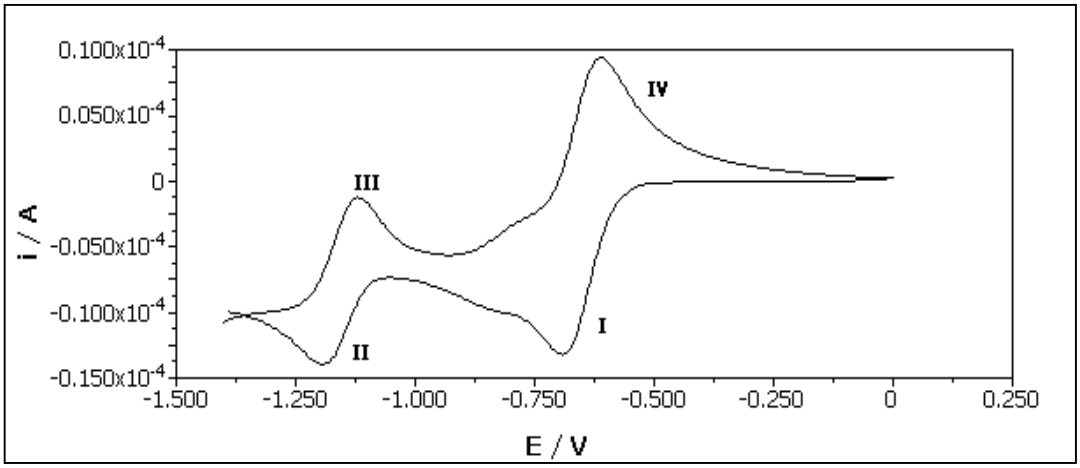

Figure 11 Cyclic voltammogram of 1.0 x 10^{-3} M 1,8-dihydroxyanthraquinone at GCE in 50 mL CH_3CN containing 0.1 M TBAP as supporting electrolyte with scan rate of 120 mV s^{-1}.

3.7 Electrochemical behavior of 1,4-benzoquinone at glassy carbon electrode

Cyclic voltammogram of 1,4–benzoquinone solution was performed in the potential window of 0.000 to -2.000V vs Ag/AgCl. 1,4–benzoquinone exhibits two redox couples as in Figure 12. The first redox couple occurs at Epc_1 = -0.636 V with Ipc_1 = 1.464 x 10^{-4} A and Epa_1 = -0.245 V with Ipa_1 = 1.366 x 10^{-4} A. The second redox couple occurs at Epc_2 = -1.231 V/Ipc_2 = 9.863 x 10^{-5} A and Epa_2 = -0.787 V with Ipa_2 = 8.329 x 10^{-5} A. The ΔEp (391 mV) is rather higher than the theoretical value (ΔEp = 59 mV), implying that the slow

electron transfer causes the peak separation to increase. The first couple (I and IV) occurs at $E^{0'}_{1}$ = -0.441 V vs Ag/AgCl. The first reduction of 1,4–benzoquinone to its semiquinone ($Q^{\cdot -}$) in CH_3CN is chemically reversible (Ipa_1/Ipc_1 = 0.933) and semiquinone can be reduced to form quinone in second reduction step.

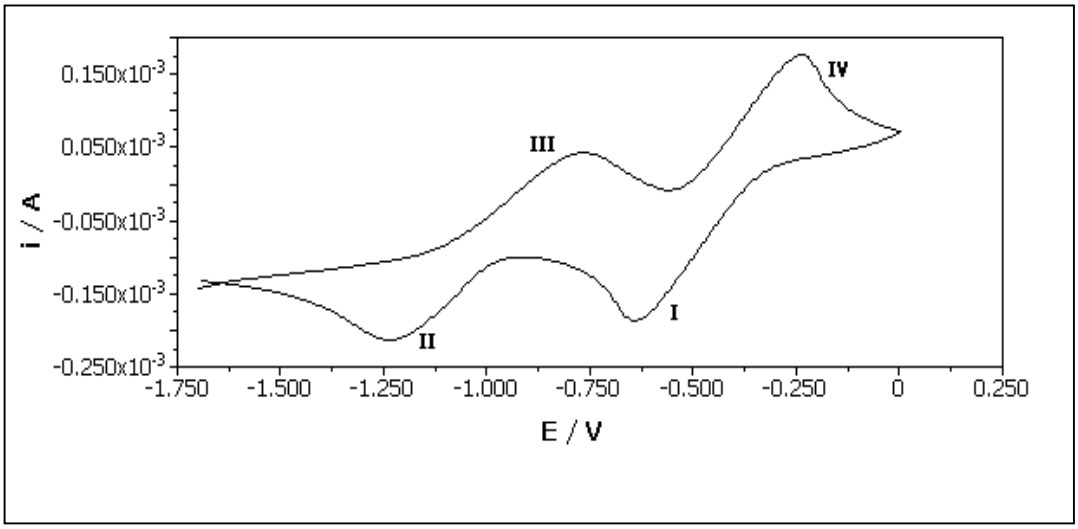

Figure 12 Cyclic voltammogram of 1.0 x 10^{-3} M 1,4-benzoquinone at GCE in 50 mL CH_3CN containing 0.1 M TBAP as supporting electrolyte with scan rate of 120 mV s^{-1}.

3.8 Electrochemical behavior of 4,5-dihydroxy anthraquinone-2–carboxylic acid disodium salt at glassy carbon electrode

Cyclic voltammogram of 4,5–dihydroxyanthraqunone-2–carboxylic acid solution was performed in the potential window from -0.225 to 2.25 V vs Ag/AgCl. 4,5-dihydroxyanthraqunone-2-carboxylic acid exhibits one step of reduction which is shown in Figure 13. The reduction peak occurs at -0.965 V vs Ag/AgCl. This reduction is electrochemical irreversible and has no oxidation couple.

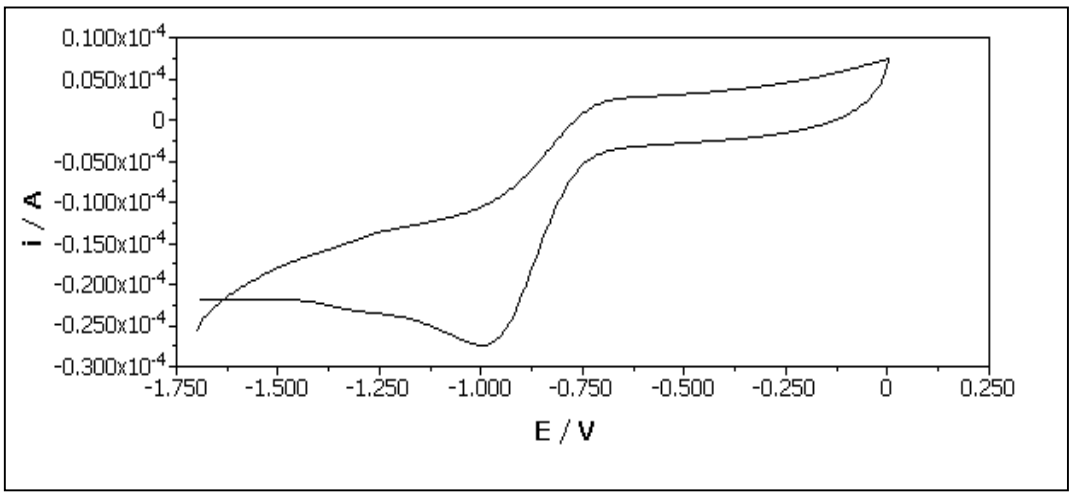

Figure 13 Cyclic voltammogram of 1.0 x 10^{-3} M 4,5-dhydroxyanthraquinone-2-carboxylic acid at GCE in 50 mL CH_3CN containing 0.1 M TBAP as supporting electrolyte with scan rate of 120 mV s^{-1}.

3.9 Conclusion about the electrochemical behavior of quinone compounds

The most of quinone compounds exhibit typical two reversible couples, except 4,5–dihydroxyanthraquinone-2-carboxylic acid. The presence of hydroxyl group helps stabilize the reduction product. It is clear from the cyclic voltammograms that the electrochemical reactions of quinone to semiquinone and quinone dianion occur in the potential range of -0.300 to -1.600 V vs Ag/AgCl. Therefore, if the quinones are to be used as modifier, the metal ions must not have any oxidation in this potential range. Cd^{2+}, with the oxidation at approximately -0.65 V; Pb^{2+}, at -0.90 V (Hu *et al*, 2003); and Zn^{2+}, at around -1.10 V depending on the modified electrodes, which can not be determined by quinone modified carbon paste electrode, consequently Cu^{2+}, at 0.1 V (Etienne *et al*, 2001); Ag^{+}, at 0.32 V (Hunag *et al*, 1994); and Hg^{2+}, at about 0.28 V (Aleixo *et al*, 1993). As a served in the preliminary studies, these three metals were selected, especially the stripping peaks by cyclic voltammetry.

3.10 Cyclic voltammetry of silver(I), mercury(II) and copper(II) at glassy carbon electrode

The cyclic voltammetric response of Ag(I) at glassy carbon electrode are shown in Figure 14. These voltammograms were obtained with a GCE immersed in 1 mM Ag(I) containing CH_3CN and 0.1 M TBAP as supporting electrolyte. The oxidation peak appears at 0.345 V and Ipa = 1.101×10^{-4} A. When the scan was reversed, the reduction peak occur at 0.160 V and Ipc = 1.310×10^{-5} A. The scan started at 1.000 V which was negative enough to drive the reduction of Ag^+ (aq) + e^- $\rightarrow$Ag(s). Silver ion in the solution takes an electron and becomes elemental Ag at the surface of working electrode. After that the oxidation reaction Ag(s) $\rightarrow$$Ag^+$(aq) + e^- occurs when the potential scan is started. Silver atom loses electron to become Ag^+(aq) back into the solution.

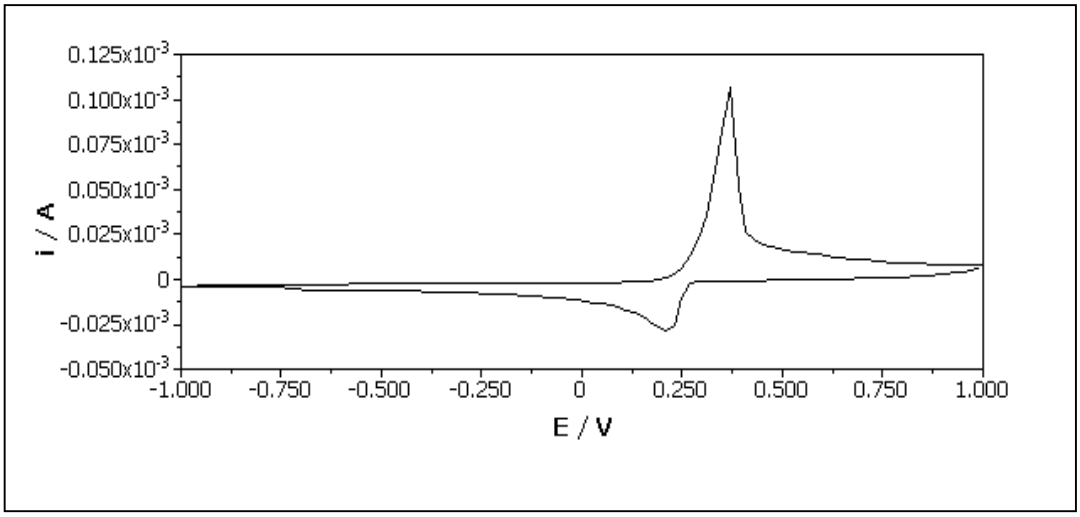

Figure 14 Cyclic voltammogram of 1.0×10^{-3} M Ag(I) at GCE in 50 mL CH_3CN containing 0.1 M TBAP as supporting electrolyte with scan rate of 120 mV s^{-1}.

Cyclic voltammogram of Hg(II) in CH_3CN containing 0.1 M TBAP as electrolyte is shown in Figure 15. The oxidation peak appears at 0.75 V and Ipc = 4.535×10^{-5} A. When the scan started at -1.500 V which is negative enough to drive the reduction of mercury species [Hg_2^{2+}(aq) + $2e^-$ $\rightarrow$ $2Hg^0$ (aq)]. Mercury ion in the solution takes two electrons and becomes Hg^0 at the surface of working electrode. After that the oxidation reaction of adsorbed

mercury was occurs [$2Hg^{0}$ (aq) $\rightarrow$ Hg_2^{2+}(aq) + $2e^{-}$]. Mercury atom losses electron to become Hg^{2+}(aq) back to the solution.

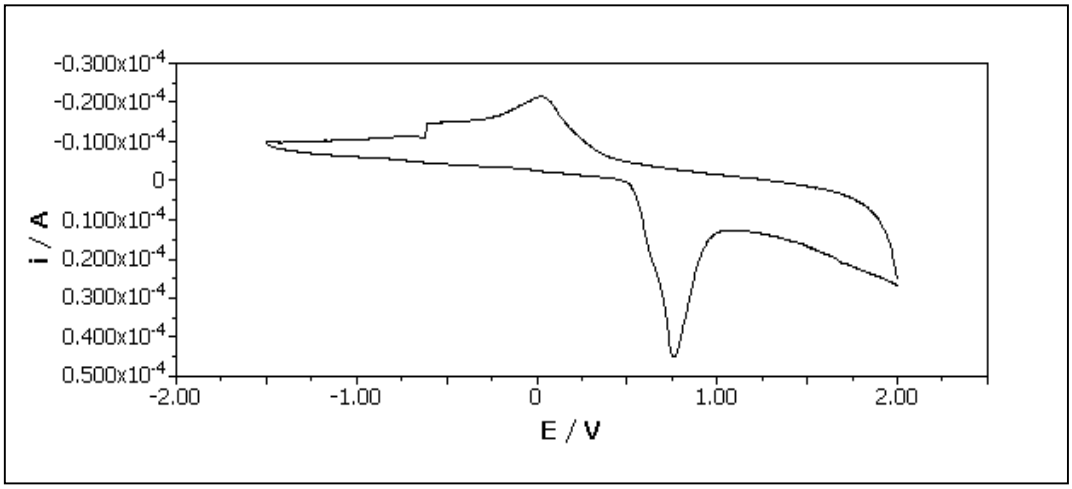

Figure 15 Cyclic voltammogram of 1.0 x 10^{-3} M Hg(II) at GCE in 50 mL CH_3CN containing 0.1 M TBAP as supporting electrolyte with scan rate of 120 mV s^{-1}.

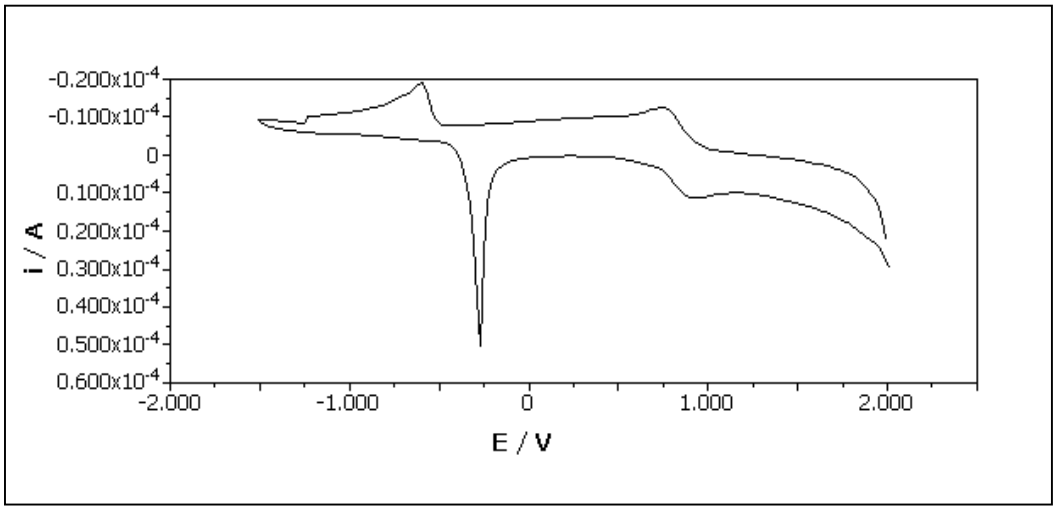

Figure 16 Cyclic voltammogram of 1.0 x 10^{-3} M Cu(II) at GCE in 50 mL CH_3CN containing 0.1 M TBAP as supporting electrolyte with scan rate of 120 mV s^{-1}.

Cyclic voltammogram of Cu(II) in CH_3CN at glassy carbon electrode is shown in Figure 16. The first reduction peak appears at 0.719 V and Ipc_1 = 4.942 x 10^{-6} A. The second

reduction peak appears at -0.680 V and Ipc_2 = 7.851 x 10^{-6} A. When the scan is reversed, the first oxidation peak occurs at –0.281 V and Ipa_2 = 4.699 x 10^{-5} A. The second oxidation peak occur at 0.899 V and Ipa_1 = 4.82 x 10^{-6} A. The scan is started at -1.75 V, which is negative enough to drive the reduction of copper(II) and becomes copper(I) [$Cu^{2+}(aq) + e^- \longrightarrow Cu^+(aq)$]. This is followed by the second reduction of copper(I) and becomes copper(0) [$Cu^+(aq) + e^- \longrightarrow Cu^0(s)$]. After that the first oxidation reaction of copper(0) and becomes copper(I) [$Cu^0(s) \longrightarrow Cu^+ + e^-$], following the second oxidation of copper(I) and becomes copper(II) back to the solution [$Cu^+(aq) \longrightarrow Cu^{2+}(aq) + e^-$].

3.11 Cyclic voltammogram of Ag(I), Cu(II) and Hg(II) at carbon paste electrode modified with quinone compounds

Cyclic voltammogram of Ag(I) at carbon paste electrode modified with quinone compounds (0.550 g of graphite powder, 0.35 g of quinone and 0.30 mL of liquid paraffin). The concentration of Ag(I) as 1.0 x 10^{-4} M in 0.2 M HNO_3 was used throughout the measurement. The voltammetric responses of Ag(I) were measured after at 5 min preconcentration time at -0.200 V preconcentration potential, 5 s equilibrate time and scan rate 80 mV s^{-1}. The current from stripping voltammogram of Ag(I) on unmodified CPE was compared with the modified CPE with various quinone compound as shown in Table 4. It is clear that the unmodified carbon paste electrode displays little peak when compared with CPE modified with 1,8-DHAQ which has significant peak as shown in Figure 17. The stripping of Ag(I) occurs at 0.350 V.

Cyclic voltammograms of 1.0 x 10^{-3} M Hg(II) in 0.001 M HNO_3 at CPE modified with quinone compounds and unmodified were run at the same condition as that of Ag (I). The potential scan was set between -2.000 V to 0.800 V with 80 mV s^{-1} scan rate. The responses of current from voltammograms on unmodified CPE are shown in Table 5. All quinone compounds used for modified carbon paste electrode shows less peak current. Therefore, there are less sensitive for Hg(II).

Cyclic voltammograms of 0.001 M Cu(II) in 0.1 M HNO_3 at CPE modified with quinone compounds and unmodified were measured at the same condition that of Ag(I). The potential scan was set between -0.200 V to 0.600 V with 80 mV s^{-1} scan rate. The responses

of current from voltammograms on unmodified CPE compared with the modified CPE are shown in Table 6. All quinone compounds were used for modified carbon paste electrode cause lower peak current when compared with unmodified electrode, except 1,8-DHAQ which is rather sensitive with Cu(II).

Table 4 The currents from stripping voltammogram of Ag(I) at various quinone compounds

Quinone compounds	Epc (V)	Current (A)			Mean ± SD
		1st	2nd	3rd	
Unmodified-CPE	0.419	6.727×10^{-5}	8.035×10^{-5}	8.141×10^{-5}	$(7.634 \pm 0.788) \times 10^{-5}$
1,5-dihydroxy-anthraquinone	0.458	5.817×10^{-5}	6.087×10^{-5}	6.085×10^{-5}	$(5.996 \pm 0.155 \times 10^{-5}$
1,4-benzoquinone	0.385	5.940×10^{-5}	7.974×10^{-5}	7.972×10^{-5}	$(7.295 \pm 0.117) \times 10^{-5}$
4,5-dihydroxy-anthraquinone-2-carboxylic acid	0.385	7.343×10^{-5}	8.061×10^{-5}	8.012×10^{-5}	$7.678 \pm 0.473) \times 10^{-5}$
1,2-dihydroxy-anthraquinone	0.419	6.701×10^{-5}	6.368×10^{-5}	6.390×10^{-5}	$(6.535 \pm 0.235) \times 10^{-5}$
1,4-dihydroxy-anthraquinone	0.429	6.244×10^{-5}	7.135×10^{-5}	6.390×10^{-5}	$(6.590 \pm 0.478) \times 10^{-5}$
1,8-dihydroxy-anthraquinone	0.347	8.720×10^{-4}	8.952×10^{-4}	8.510×10^{-4}	$(8.615 \pm 0.148) \times 10^{-5}$
Anthraquinone	0.487	2.902×10^{-5}	2.723×10^{-5}	2.824×10^{-5}	$(2.813 \pm 0.127) \times 10^{-5}$

Table 5 The current from stripping voltammogram of Hg(II) at various quinone compounds

Quinone compounds	Epc (V)	Current (A)			Mean ± SD
		1st	2nd	3rd	
Unmodified-CPE	0.42	4.344×10^{-4}	5.887×10^{-4}	6.120×10^{-4}	$(5.450 \pm 0.965) \times 10^{-4}$
1,5-dihydroxy-anthraquinone	0.43	4.772×10^{-4}	5.390×10^{-4}	5.612×10^{-4}	$(5.258 \pm 0.435) \times 10^{-4}$
1,4-benzoquinone	0.56	3.134×10^{-4}	4.121×10^{-4}	4.512×10^{-4}	$(3.922 \pm 0.710) \times 10^{-4}$
4,5-dihydroxy-anthraquinone-2-carboxylic acid	0.51	5.850×10^{-4}	6.340×10^{-4}	6.928×10^{-4}	$(6.373 \pm 0.540) \times 10^{-4}$
1,2-dihydroxy-anthraquinone	0.52	3.354×10^{-4}	4.006×10^{-4}	5.121×10^{-4}	$(4.160 \pm 0.894) \times 10^{-4}$
1,4-dihydroxy-anthraquinone	0.44	2.972×10^{-4}	3.091×10^{-4}	4.221×10^{-4}	$(3.428 \pm 0.689) \times 10^{-4}$
1,8-dihydroxy-anthraquinone	0.42	5.441×10^{-4}	6.117×10^{-4}	6.214×10^{-4}	$(5.779 \pm 0.478) \times 10^{-4}$
Anthraquinone	0.44	3.759×10^{-4}	4.213×10^{-4}	4.311×10^{-4}	$(4.094 \pm 0.295) \times 10^{-4}$

Table 6 The current from stripping voltammogram of Cu(II) at various quinone compounds

Quinone compounds	Epc (V)	Current (A)			Mean ± SD
		1st	2nd	3rd	
Unmodified-CPE	0.233	4.148×10^{-4}	4.003×10^{-4}	4.100×10^{-4}	$(4.084 \pm 0.073) \times 10^{-4}$
1,5-dihydroxy-anthraquinone	0.242	3.726×10^{-4}	3.490×10^{-4}	3.478×10^{-4}	$(3.565 \pm 0.140) \times 10^{-4}$
1,4-benzoquinone	0.219	1.676×10^{-4}	1.629×10^{-4}	1.753×10^{-4}	$(1.686 \pm 0.063) \times 10^{-4}$
4,5-dihydroxy-anthraquinone-2-carboxylic acid	0.224	1.552×10^{-4}	2.280×10^{-4}	2.270×10^{-4}	$(2.034 \pm 0.417) \times 10^{-4}$
1,2-dihydroxy-anthraquinone	0.214	2.305×10^{-4}	2.309×10^{-4}	2.401×10^{-4}	$(2.338 \pm 0.054) \times 10^{-4}$
1,4-dihydroxy-anthraquinone	0.224	1.928×10^{-4}	2.821×10^{-4}	2.511×10^{-4}	$(2.420 \pm 0.453) \times 10^{-4}$
1,8-dihydroxy-anthraquinone	0.419	5.441×10^{-4}	6.117×10^{-4}	6.214×10^{-4}	$(5.924 \pm 0.421) \times 10^{-4}$
Anthraquinone	0.273	1.179×10^{-4}	1.257×10^{-4}	1.321×10^{-4}	$(1.218 \pm 0.055) \times 10^{-4}$

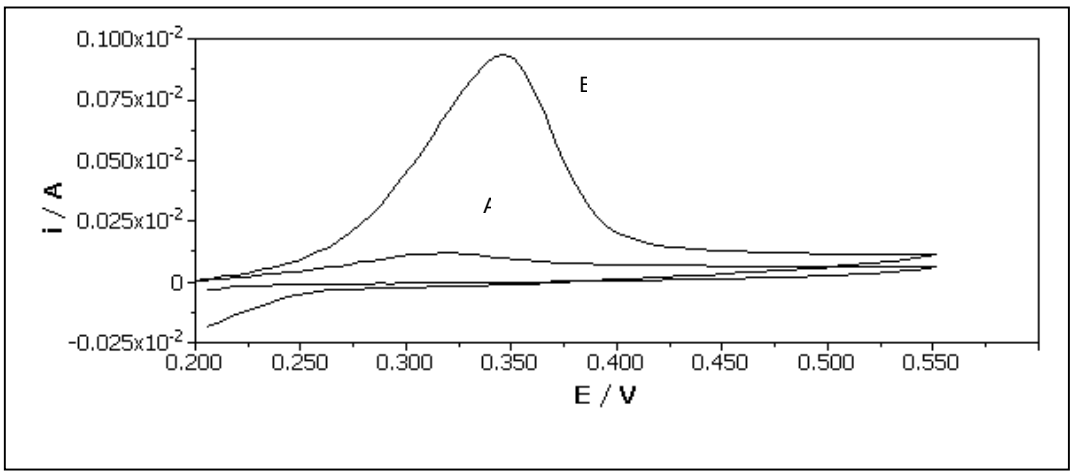

Figure 17 Stripping voltammogram of 1.0 x 10^{-4} M Ag(I) at unmodified (A) and modified electrode with 1,8-dihydroxyanthraquinonn (B) in 0.2 M HNO_3 for 5 min preconcentration time and scan rate of 80 mV s^{-1}.

3.12 Comparison of stripping voltammogram of Ag(I) between differential pulse and square wave mode

Stripping voltammogram of 1.0 x 10^{-4} M Ag(I) in differential pulse mode at carbon paste electrode modified with 1,8–DHAQ occur at 0.40 V. It displays 2.25 x10^{-3} A of current peak. For the square wave mode, the stripping voltammogram of Ag(I) occurs at 0.39 V and it has 3.22 x 10^{-3} A of current peak. Figure 18 displays the stripping curves of Ag(I) in differential pulse and square wave mode. In square wave mode, a sharp oxidation peak appears. Therefore, the sensitivity of SWASV proved to be better than that of DPASV. The square ware currents are higher than the differential pulse response (Wang, 2000).

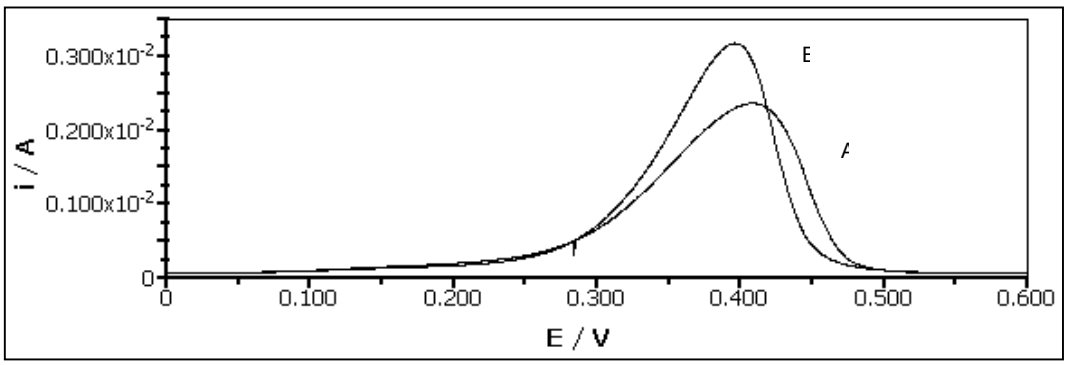

Figure 18 Differential pulse stripping voltammogram (A) and square wave stripping voltammogram (B) of Ag(I) for 1.0 x 10^{-4} M in 0.2 M HNO_3 after deposition time of 5 min at -0.20 V vs Ag/AgCl double junction reference electrode**.**

3.13 Stripping voltammogram of Ag(I) and Cu(II) at CPE modified with 1,8–DHAQ

The simultaneous determination of Cu(II) and Ag(I) in 0.2 M HNO_3 solution was carried out by SWASV and the voltammogram are shown in Figure 19. Two well defined stripping peaks are observed at the 1,8–dihydroxyanthraquinone modified carbon paste electrode. The result indicates that 1,8–dihydroxyanthraquinone can greatly promote the preconcentration of Cu(II) and Ag(I) at the carbon paste electrode and significantly increase the sensitivity of the determination of Cu(II) and Ag(I). The large difference of stripping peak potential between Cu(II) and Ag(I) suggests the possibility of the simultaneous determination of Cu(II) and Ag(I) in the HNO_3 solution by using SWASV at the 1,8–dihydroxyanthraquinone modified carbon paste electrode. But after investigation of redox potential for 1,8–dihydroxyanthraquinone from previous section indicated that the redox peak potential of 1,8–dihydroxyanthraquinone locating in the same potential range as that of stripping peak of Cu (II). Therefore, Cu(II) can not be determined by 1,8–DHAQ modified carbon paste electrode.

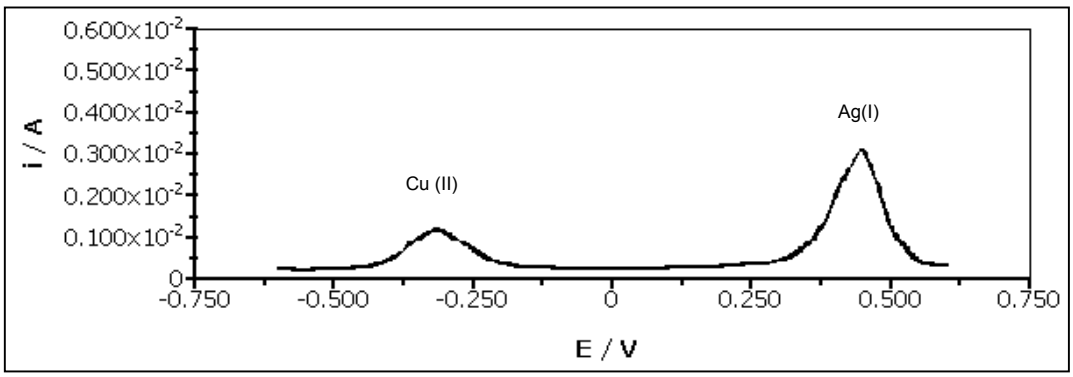

Figure 19 Simultaneous stripping voltammogram of 1.0 x 10^{-3} M Cu^{2+} and Ag^{+} in 0.1 M HNO_3 at CPE-1,8-DHAQ, preconcentration time of 5 min at -0.20 V with 50 mV of pulse amplitude, 5 mV step potential and 100 Hz of frequency.

3.14 Comparison of stripping voltammogram of Ag(I) at Ag/AgCl with Ag/AgCl double junction reference electrode

Stripping voltammogram of 1.0 x 10^{-4} M Ag(I) in 0.2 M HNO_3 at carbon paste electrode modified with 1,8–DHAQ occurs at 0.426 V. The using of Ag/AgCl as reference electrode, the peak current of Ag(I) was 2.40 x 10^{-3} A at Ag/AgCl reference electrode. The peak current of Ag(I) at Ag/AgCl double junction reference electrode was 2.81 x 10^{-3} A. Ag/AgCl with 3 M KCl was leading chloride ions into solution, therefore the current peak of Ag(I) is decreased due to the formation of AgCl (Li and Liu, 2001). The Ag/AgCl double junction reference electrode has 3 M KCl as inner solution and 3 M $NaNO_3$ as other solution, the stripping is higher because $NaNO_3$ as a bridge solution and vigor frits is used at the end of the salt bridge to avoid an in flux of chloride ions. The stripping voltammograms of Ag(I) at different reference electrode are shown in Figure 20.

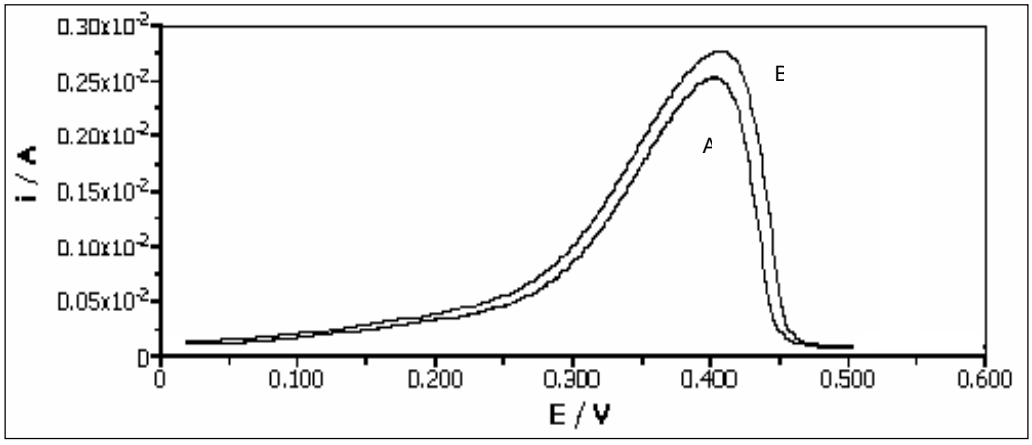

Figure 20 Stripping voltammogram of 1.0 x 10^{-4} M Ag(I) in 0.2 M HNO_3 ; Ag/AgCl reference electrode (A) and Ag/AgCl double junction reference electrode (B). Other working conditions are as in Figure 19.

3.15 Cyclic voltammetry of Ag(I) at CPE modified with 1,8–DHAQ for various scan rates

Carbon paste electrode modified with 1,8–DHAQ used as working electrode, the solution of silver 1.0 x 10^{-4} M in 0.2 M HNO_3 was measured with various scan rate. The results are shown in Table 7. Figure 21 displays the relation between square root of scan rate and the reduction current and the oxidation current of silver (Randles–Sevcik equation). Both reduction and oxidation peak of Ag(I) can be considered tend to be diffusion controlled at higher scan rate. At lower scan rate, a nonlinear relationship between peak current and square root of scan rate is obtained due to the deposited of silver on the electrode surface. The plot of Ipc and Ipa are tend to straight curved at higher scan rates, indicating that the process is diffusion controlled. A shift of potentials is observed with increasing scan rate. This implies that the chemical step proceeds electron transfer. The non–zero intercept is caused by non faradic current contributing toward the overall peak current (Monk, 2001).

Table 7 The data of the current peaks and square root of scan rate for Ag(I)

Scan rate ($mV\ s^{-1}$)	Square root of scan rate $(mV^{-1})^{1/2}$	Ipa	Ipc	Epa	Epc
25	5	9.284×10^{-5}	3.342×10^{-4}	0.168	0.335
50	7.07	4.369×10^{-4}	1.355×10^{-4}	0.164	0.338
100	10	2.790×10^{-4}	7.920×10^{-4}	0.152	0.409
200	14.14	3.536×10^{-4}	9.667×10^{-4}	0.135	0.427
400	20	4.740×10^{-4}	1.136×10^{-3}	0.108	0.453
600	24.49	5.121×10^{-4}	1.156×10^{-3}	0.095	0.471
800	28.28	5.962×10^{-4}	1.221×10^{-3}	0.018	0.502

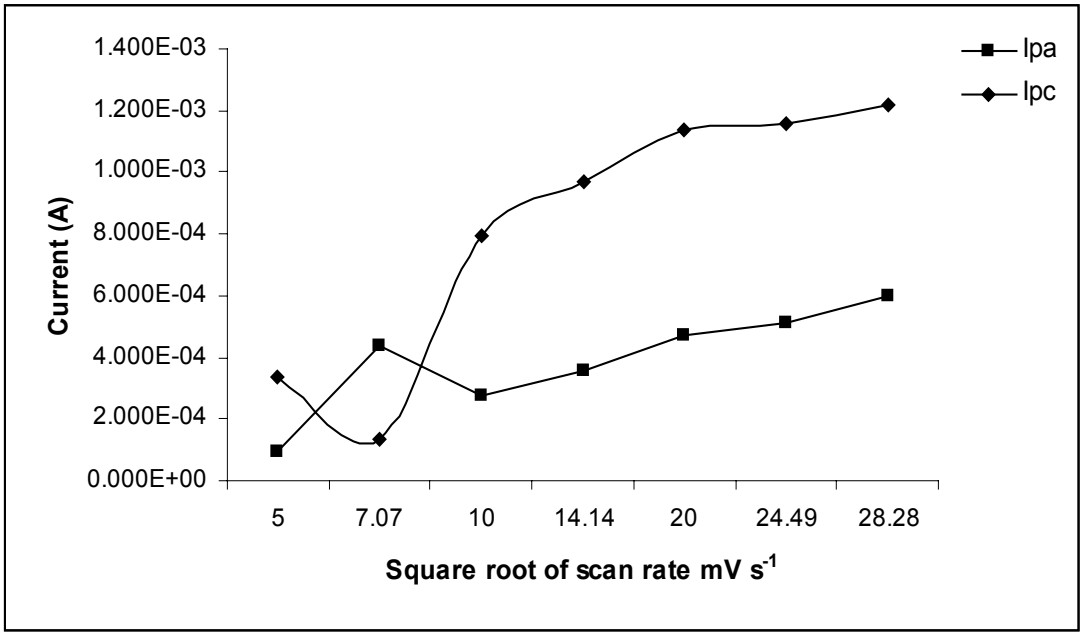

Figure 21 The plotting between square root of scan rate with the reduction current (Ipc) and the oxidation current (Ipa)

3.16 Operational principle

The method to increase the sensitivity of a carbon paste electrode is the making use of modified electrode which is able to preconcentrate the silver ions from aqueous solution on to electrode surface by interaction with 1,8–DHAQ as a ligand. In the preconcentration step, the silver ion is chemically deposited at the electrode surface under carefully controlled conditions. The deposited silver is then electrochemically stripped off and the peak current was measured by voltammetric methods. The performance of newly developed 1,8–DHAQ modified carbon paste electrode is use on the preconcentration of Ag^{+} from aqueous solution onto the surface of the modified electrode by forming complexes with the modifier. The formation of the complex of 1,8–DHAQ with silver ion exhibits 1:2 (Ag:1,8–DHAQ) stoichiometry (Photicunapat, 2005). The surface concentration of Ag^{+} is much larger than that of the unmodified carbon paste electrode, and the sensitivity is greatly increased. The preconcentrated of Ag^{+} was reduced at -0.25 V and the products were then oxidized in the stripping step. The mechanism can be described as follows:

$(Ag^{+})_{solution} + (1,8\text{–DHAQ})_{surface} \rightarrow (Ag^{+}\text{-}1,8\text{–DHAQ})_{adsorption}$

[the preconcentration step];

$(Ag^{+}\text{-}1,8\text{–DHAQ})_{adsorption} + e^{-} \rightarrow (Ag^{0}\text{–}1,8\text{–DHAQ})_{adsorption}$

[the reduction step];

$(Ag^{0}\text{–}1,8\text{–DHAQ})_{adsorption} \rightarrow (Ag^{+})_{solution} + (1,8\text{–DAHQ})_{surface} + e^{-}$

[the stripping step]

3.17 Optimization for the conditions for silver(I) analysis

3.17.1 The paste composition

The quantity of 1,8–DHAQ in the carbon paste is expected to significantly influence the height of the voltammetric signal. Seven compositions of the 1,8–DHAQ modified electrode were studied and the results are summarized in Table 8 and Table 9. The experiments were performed under conditions as follows: 1.0×10^{-4} and 0.5×10^{-4} M Ag^{+} preconcentration solution, 5 min preconcentration time and 0.2 M HNO_3 as electrolysis and stripping media. The

experiments performed on the unmodified carbon paste electrode did not yield any voltammetric responses (current) for Ag^{+}, indicating that the conductive matrix (carbon graphite) was inert with respect to silver adsorption. When the weight of graphite and oil was kept constant at 0.275 g and 0.15 ml respectively, the weight of 1,8–DHAQ was increased from 0.025 to 0.175 g. The stripping peak of Ag(I) increases and the high current and the best standard deviations was obtained at 0.050 g of 1,8–DHAQ. The increase in the amount of 1,8–DHAQ from 0.075 g to 0.175 g has led to a decrease in the electrode responses as shown in Figure 22. This is possibly due to the decrease in the conductance of the electrode composition with increasing the amount of 1,8–DHAQ. The weight of 0.275 g graphite and 0.050 g 1,8–DHAQ was therefore selected to be optimum condition for the next experiments.

When the volume of pasting liquid (mineral oil, liquid paraffin and silicone oil) was increased from 0.15 to 0.30 mL, the obtained results are show in Table 10–12. The highest peak current was obtained with liquid paraffin as pasting liquid. The hydrophobicity of the electrode surface was increased and hence the decrease in the surface reaction between the metal ions and the functional ligand (Etienne, 2001). The increases of the pasting liquid content decreasing electron transfer rate (Wang, 2000). There the optimum electrode composition was 0.275 g graphite powder, 0.050 g 1,8–DHAQ and 0.15 mL liquid paraffin.

Table 8 The data of the current peaks of 1.0 x 10^{-4} M Ag(I) at various paste compositions

1,8-DHAQ (g)	Current (mA)											
	1st	2nd	3rd	4th	5th	6th	7th	8th	9th	10th	Mean	SD
0.025	2.01	2.59	3.03	3.34	2.38	2.93	2.33	2.73	2.71	2.48	2.65	0.384
0.050	3.66	3.54	3.52	3.41	3.61	3.55	3.50	3.61	3.71	3.59	3.57	0.085
0.075	2.91	3.46	3.35	3.68	3.14	3.40	3.64	3.30	3.39	3.40	3.37	0.223
0.100	3.24	3.10	3.45	2.78	3.52	2.95	3.14	2.96	3.38	3.00	3.15	0.242
0.125	3.14	3.34	3.39	3.45	2.91	2.96	3.10	3.00	3.59	3.11	3.20	0.229
0.150	2.73	2.69	2.75	3.26	3.37	2.85	3.14	2.69	3.19	3.11	2.98	0.262
0.175	2.73	2.84	2.87	2.61	3.12	2.85	2.86	2.79	2.61	2.72	2.80	0.149

Table 9 The data of the current peaks of 0.5 x 10^{-4} M Ag(I) at various paste compositions

1,8-DHAQ (g)	Current (mA)											
	1st	2nd	3rd	4th	5th	6th	7th	8th	9th	10th	Mean	SD
0.025	1.33	1.39	1.41	1.37	1.61	1.45	1.49	1.63	1.38	1.51	1.46	0.10
0.050	1.62	1.64	1.69	1.45	1.74	1.62	1.59	1.66	1.71	1.54	1.63	0.09
0.075	1.50	1.67	1.51	1.63	1.44	1.71	1.44	1.72	1.56	1.53	1.57	0.11
0.100	1.41	1.70	1.34	1.76	1.54	1.62	1.52	1.53	1.63	1.52	1.56	0.13
0.125	1.41	1.61	1.55	1.53	1.34	1.74	1.52	1.52	1.56	1.64	1.54	0.11
0.150	1.50	1.51	1.58	1.43	1.77	1.35	1.65	1.50	1.42	1.61	1.53	0.12
0.175	1.39	1.40	1.47	1.45	1.47	1.61	1.41	1.52	1.71	1.59	1.50	0.10

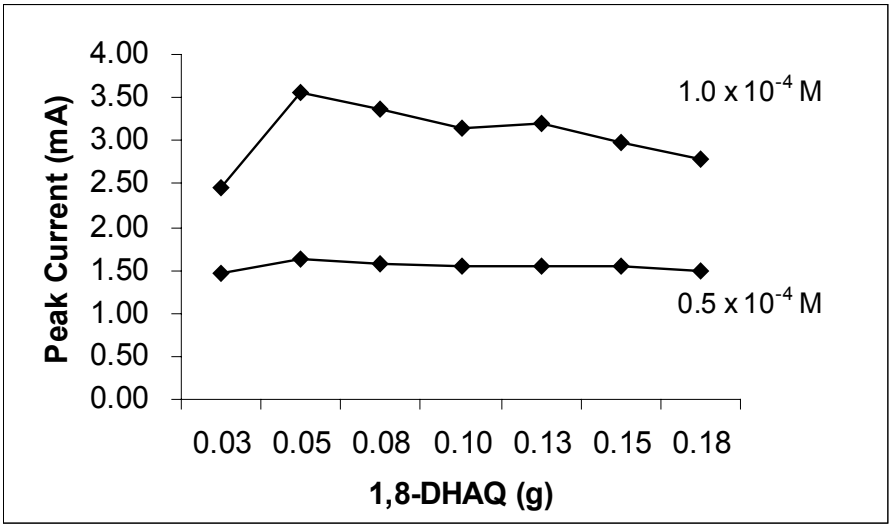

Figure 22 Effects of the content of 1,8-DHAQ in carbon paste mixture (comparing with 0.275 g of graphite powder) on stripping peak currents of 0.5 x 10^{-4} and 1.0 x 10^{-4} M Ag(I) in 0.2 M HNO_3 with 5 min preconcentration time at -0.20 V with 50 mV of pulse amplitude, 5 mV step potential and 100 Hz of frequency.

Table 10 The currents at various volumes of mineral oil with the constant amount of graphite powder 0.275 g and 1,8-DHAQ 0.050 g.

Volume	Current (mA)				
(mL)	1st	2nd	3rd	Mean	SD
0.15	1.35	2.50	3.88	2.577	1.206
0.20	4.42	3.99	4.20	4.203	0.302
0.25	4.12	4.15	4.83	4.367	0.256
0.30	4.44	4.38	4.43	4.417	0.032

Table 11 The peak currents at various volumes of liquid paraffin with the constant amount of graphite powder 0.275 g and 1,8-DHAQ 0.050 g.

Volume	Current (mA)				
(mL)	1st	2nd	3rd	Mean	SD
0.15	5.54	5.50	5.56	5.533	0.031
0.20	5.24	5.04	5.07	5.117	0.108
0.25	3.62	4.01	5.03	4.220	0.728
0.30	3.60	3.89	4.45	3.980	0.432

Table 12 The peak currents at various volumes of silicone oil with the constant amount of graphite powder 0.275 g and 1,8-DHAQ 0.050 g.

Volume	Current (mA)				
(mL)	1st	2nd	3rd	Mean	SD
0.15	2.96	3.56	4.69	3.737	0.878
0.20	3.6	4.4	4.79	4.263	0.607
0.25	3.66	4.04	4.38	4.027	0.360
0.30	2.65	3.11	4.01	3.267	0.692

3.17.2 Electrolyte solution

Electrochemical techniques are commonly carried out in a media that consists of an electrolyte. Electrolyte solutions are required in controlled potential experiments in order to decrease the resistance of the solution, to eliminate electromigration effects, and to maintain a constant ionic strength (Wang, 2000). Ag^{+} has different electrochemical behavior in different electrolytes. With this view, various electrolytes were evaluated for their suitability in acute emulating Ag^{+} at the electrode surface. Table 13 gives a general overview of the SWASV electrochemical responses of Ag(I) in different electrolytes. The choice of the electrolyte selected in Table 13 is governed by two reasons. The first one, comparison with previous studies (Hunag, 1994). The second, a large pH range to correspond to the dissolution steps of the various materials containing silver. The effects of some electrolytes, such as $Na_2B_4O_7$, H_3PO_4, $HClO_4$, HNO_3, KH_2PO_4, Na_2HPO_4, $NaClO_4$, $NaNO_3$, $NaCOOCH_3$ and CH_3COONH_4 on stripping peak currents of Ag^{+} were studied. Among the tested ones, $HClO_4$, HNO_3, and $NaNO_3$ were found to be the best for this purpose. Therefore, various concentrations of this electrolyte were investigated. The good stripping peaks of acid solution were obtained with 0.1 M $HClO_4$ and 0.2 M HNO_3, however, The most effective silver detection was accomplished by performing both preconcentration and stripping in 0.8 M $NaNO_3$ solution. Increasing the concentration of $NaNO_3$ solution from 0.3 to 1.2 M (Figure 23) which significantly improve the sensitivity of silver detection but the concentration of $NaNO_3$ in the range of 0.9 to 1.2 M provided increasing of back ground current and broad of peak. Therefore, 0.8 M $NaNO_3$ is recommended as preconcentration and stripping media due to they have the largest stripping peak current, the low background current (Figure 24) and the best peak shape.

Table 13 Electrochemical response of silver in various electrolytes at CPE-1,8-DHAQ

Electrolyte	pH	Concentration	Current (mA)			
		(M)	1st	2nd	3rd	Mean
$Na_2B_4O_7$	9.22	0.2	0.828	0.786	0.924	0.846
H_3PO_4	1.50	0.2	1.68	1.84	1.76	1.760
$HClO_4$	2.31	1.00×10^{-4}	0.279	0.291	0.273	0.281
$HClO_4$	2.19	1.00×10^{-3}	0.357	0.329	0.341	0.342
$HClO_4$	1.81	0.01	0.835	0.856	0.846	0.846
$HClO_4$	1.04	0.10	2.62	2.43	2.51	2.520
$HClO_4$	1.02	0.20	1.66	1.75	1.81	1.740
$HClO_4$	1.01	0.30	1.17	1.09	1.14	1.133
HNO_3	1.88	0.05	2.31	2.44	2.26	2.337
HNO_3	0.97	0.15	3.26	3.19	3.22	3.223
HNO_3	0.82	0.20	3.63	3.42	3.46	3.503
HNO_3	0.63	0.30	0.831	0.857	0.839	0.842
KH_2PO_4	4.50	0.20	1.67	1.71	1.69	1.690
Na_2HPO_4	8.21	0.20	1.17	1.25	1.31	1.243
$NaClO_4$	5.77	0.20	2.11	2.25	2.29	2.217
$NaNO_3$	6.01	0.20	2.61	2.47	2.73	2.603
$NaNO_3$	5.98	0.40	2.92	3.34	3.45	3.237
$NaNO_3$	5.94	0.50	4.43	4.66	4.72	4.603
$NaNO_3$	5.90	0.60	5.08	5.21	5.33	5.207
$NaNO_3$	5.87	0.70	5.69	5.81	5.51	5.670
$NaNO_3$	5.83	0.80	6.13	6.04	6.11	6.093
$NaNO_3$	5.81	0.90	6.27	6.34	6.13	6.247
$NaNO_3$	5.79	1.00	6.82	6.76	6.91	6.830
$NaNO_3$	5.77	1.1	6.71	7.01	7.12	6.947
$NaNO_3$	5.75	1.2	7.26	7.19	7.03	7.160
$NaCH_3COO$	6.21	0.20	1.57	1.66	1.61	1.613
$CH_3COO\ NH_4$	6.91	0.20	1.99	1.95	1.89	1.943
$CH_3COONH_4 + NaClO_4$	0.41	each 0.10	1.83	1.91	1.86	1.867

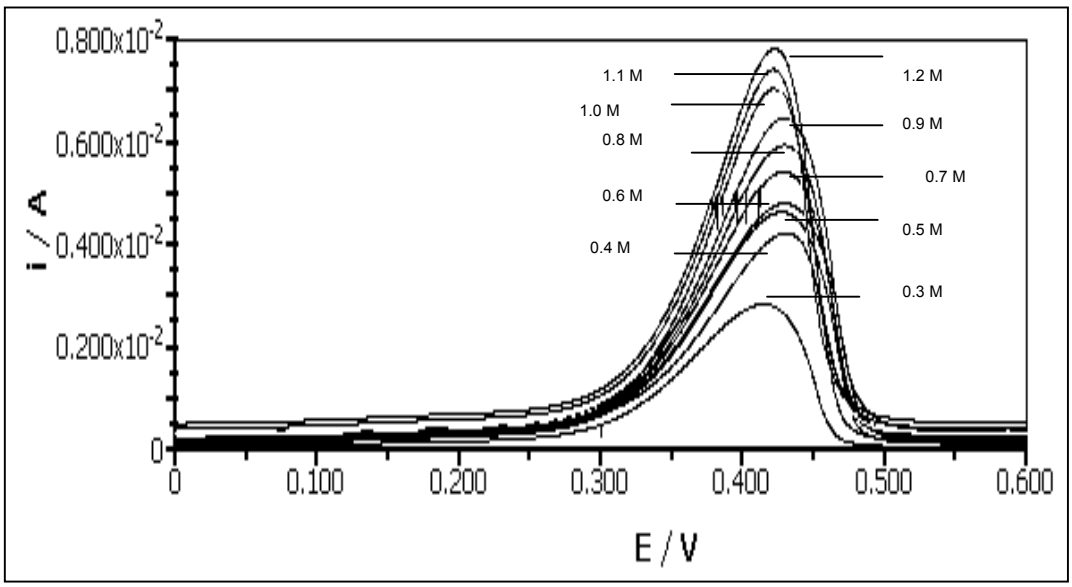

Figure 23 Stripping voltammograms of 1.0 x 10^{-4} M Ag(I) at CPE-1,8-DHAQ for 0.3 to 1.2 M of $NaNO_3$. Preconcentration time 5 min at -0.20 V with 50 mV of pulse amplitude, 5 mV step potential and 100 Hz of frequency.

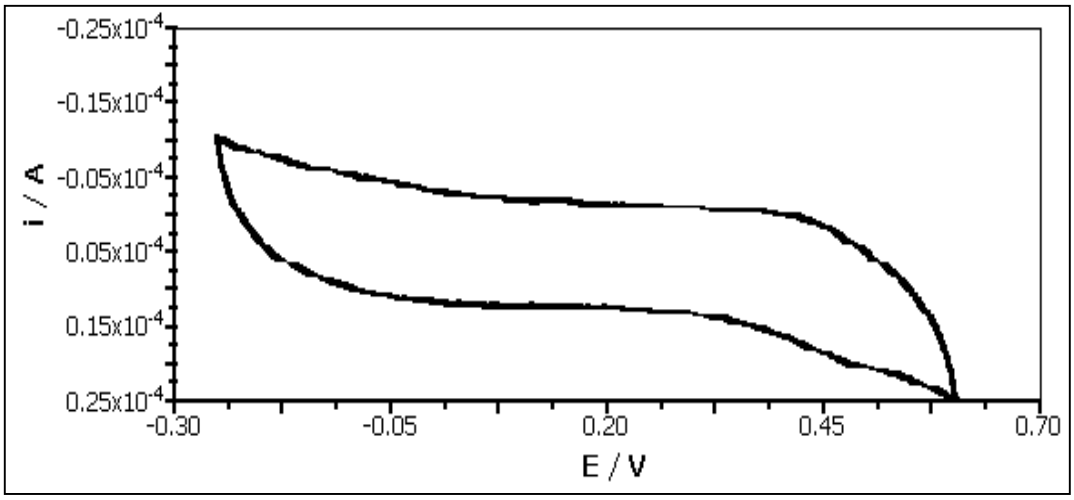

Figure 24 Blank cyclic voltammogram of $NaNO_3$ 0.8 M at CPE-1,8-DHAQ with 80 mV s^{-1} of scan rate

3.17.3 Effect of pH

Throughout the process of accumulation of the solution pH plays crucial role because of its direct effect on modifier–silver complicated equilibrium. This is important condition was studied for 0.8 M $NaNO_3$ solution in pH range of 1.00 – 9.00 with the Ag(I) concentration of 0.5 x 10^{-4} and 1.0 x 10^{-4} M. The results are summarized in Table 14-15. The Ag (I) peak current as a function of pH are shown in Figure 25. Maximum peak was observed at pH 2 and 3. Continuous increasing of pH led to a decreasing of peak current which is due to the formation of metal hydroxide complexes that are sparingly soluble. These hydroxide complexes may precipitate either on the wall of the electrolytic cell or on the electrode surface. However, the signal at pH 1 was low due to the favorable condition for leaching of the accumulated Ag(I) from Ag(I)–1,8–DHAQ complex at the surface of electrode as soon as medium was exchanged. Therefore, the optimum of pH is selected to be 2.00.

Table 14 The result of peak currents for Ag(I) 0.5 x 10^{-4} M in 0.8 M HNO_3 at pH 1.00 to 9.00

pH	Current (mA)				
	1st	2nd	3rd	Mean	SD
1.00	3.14	3.34	3.58	3.35	0.220
2.00	3.84	3.74	3.99	3.86	0.126
3.02	3.95	3.93	3.58	3.82	0.208
4.02	3.14	3.61	3.68	3.48	0.294
5.22	3.03	3.34	3.65	3.34	0.310
6.03	3.30	3.29	3.33	3.31	0.021
7.00	3.39	2.92	3.28	3.20	0.246
8.01	2.95	2.89	2.96	2.93	0.038
9.00	2.78	2.52	2.58	2.63	0.136

Table 15 The result of peak current for Ag(I) 1.0 x 10^{-4} M in 0.8 M HNO_3 at pH 1.00 to 9.00

pH	Current (mA)				
	1st	2nd	3rd	Mean	SD
1.00	5.14	5.25	5.82	5.40	0.37
2.03	6.01	6.15	6.13	6.10	0.08
3.00	5.62	5.75	5.95	5.77	0.17
4.02	5.38	5.11	5.10	5.20	0.16
5.42	4.86	5.18	5.38	5.14	0.26
6.00	4.52	4.52	4.09	4.38	0.24
7.02	4.08	4.11	4.30	4.16	0.12
8.01	3.54	3.67	3.52	3.58	0.08
9.02	2.78	3.07	2.80	2.88	0.16

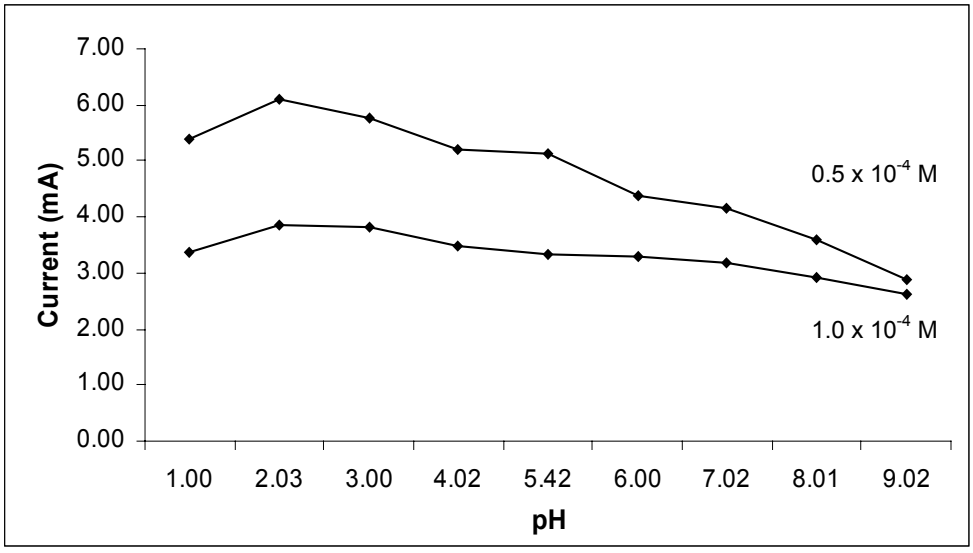

Figure 25 Effects of pH on stripping peak current of Ag^+ 0.5 x 10^{-4} and 1.0 x 10^{-4} M in HNO_3 0.8 M, preconcentration time 5 min at -0.20 V with 50 mV of pulse amplitude, 5 mV step potential and 100 Hz of frequency.

3.17.4 Activation of carbon paste electrode

The effects of surface pretreatment on CPE have been studied. A significant one was that by Rice and co – workers (Rice *et al*, 1983 cited in Motta and Guadalupe, 1994) where the effects of chemical and electrochemical oxidation in electron transfer rate of $[Fe(CN)_6]^{3-/4-}$ and hydroxyquinone were studies. For both systems the electrochemical reversibility improved upon surface activation, which was attributed to oil depletion from the surface with a concomitant increase in surface hydrophobicity. Carbon paste electrode prepared from lipophilic pasting liquids displays markedly hydrophobic character of their surface, including the so–called dry mixtures with a relatively low content of the binding results in moderately reversible or even totally irreversible behavior of redox couples at CPEs whereas the same substances measured at ordinary solid electrodes may exhibit a fair reversibility (Ravinchandran and Baldwin, 1984). In voltammetric analysis, the signals of interest are considerably shifted towards the corresponding potential limit (Rice *et al*., 1983) cited in Motta and Guadalupe, 1994).

The effect of this surface alteration which is also known as electrolytic activation (anodic – cathodic cyclic voltammetry) can advantageously be investigated using comparative measurement with activated and unactivated CPE with various procedures. The results are shown in Table 16. The procedure of Ravinchandran and Baldwin, and Motta and Guadalupe provided the highest stripping peak, but the procedure of Motta and Guadalupe displays the lowest of standard deviation. Among the various activation procedures, the method of Motta and Guadalupe was used for the activation of carbon paste electrode throughout the oxidative potential region at a relatively high scan speed during 10 min in 0.5 M $NaHCO_3$). Figure 26 indicated silver oxidation peak with the enhancement of current, and background current is lowered when compared activated and unactivated CPE. A possible discussion is that the electrochemical oxidized CPE is reduced at deposition potential and that the corresponding re-oxidation component, the paraffin removal, porosity and edge effects enhancement much greatly affect the background signal more than the silver one. Under activation of carbon particles is transformed into hydrophilic functional groups such as –C=O, -C-O^- or –C=OH^+. That is able to repel the lipophilic layer (Svancara *et al*., 1996). Thus, anodization leads to removal of lipophilic layer of pasting liquid are results in the principle changes of surface condition at CPEs. Their surface becomes hydrophilic and behaves like that of solid graphites.

T[illegible] by

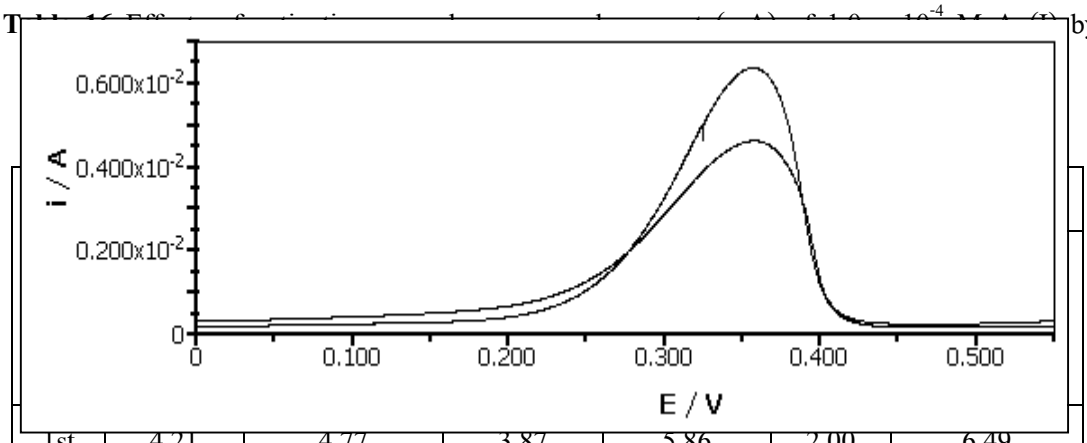

1st	4.21	4.77	3.87	5.86	2.00	6.49
2nd	4.35	6.13	4.96	5.76	5.56	6.65
3rd	4.96	6.07	4.99	5.93	5.20	6.55
4th	4.82	6.11	4.84	5.71	4.53	6.71
5th	4.89	6.14	5.54	5.65	5.33	6.68
6th	5.00	6.16	5.19	5.48	5.83	6.69
7th	4.76	6.48	5.89	5.62	5.93	6.72
8th	4.47	5.92	5.55	6.14	5.56	6.71
9th	4.37	6.68	6.23	6.15	5.10	6.67
10th	4.16	6.63	5.55	6.12	5.45	6.65
Mean	4.60	6.11	5.26	5.84	5.05	6.65
SD	0.32	0.53	0.66	0.24	1.14	0.08
RSD	6.97	8.75	12.45	4.08	22.62	1.13

Activated

Unactivate

Figure 26 The response of peak current between activated (Motta and Guadalupe, 1994) and unactivated of CPE-1,8-DHAQ at 1.0 x 10^{-4} M of Ag(I) with preconcentration time 5 min at -0.20 V with 50 mV of pulse amplitude, 5 mV step potential and 100 Hz of frequency.

3.17.5 Preconcentration time

Preconcentration time is a decisive factor in any techniques dealing with a preconcentration step. The dependence of peak current on the preconcentration time was studied for three different concentrations of Ag(I) under carefully controlled convective conditions. As would be expected, rapid convectional transport during accumulation process was essential for a sensitive determination. The result summarized in Table 17-19. Figure 27 shows the relation between peak current and concentration time for three different concentrations of Ag(I). Peak currents increased proportionally with the time from 2 to 12 min. The peak current increased linearly up to 8 min, indicating the enhancement of the accumulation of silver on the electrode surface. Longer deposition time does not significantly increase the response probably because the coverage of the active sites on 1,8-DHAQ available to silver was saturated. Beyond 8 min preconcentration time, the linear portion of the curve tends to become constant. For each of the concentration employed, the constant of peak current value was different, larger values being obtained for higher concentration of Ag(I). This is due to the fact that the maximum amount of the Ag^{+}-1,8-DHAQ complex that can be accumulated in such prolonged accumulation time is determined by equilibrium system for a complex process. This profiles of silver uptake obtained different concentrations are well in accord with the model developed to describe the kinetic and equilibrium of the accumulation process of Ag(I) in chemically modified carbon paste electrodes (Kalcher *et al*., 1995). For higher concentrations a relatively preconcentration time must be employed to avoid saturation and the subsequent non-linear between Ag(I) concentration and peak current. On the other hand, it is possible to enhance the sensitivity of the method by employing extended preconcentration periods for lower concentration of Ag(I). Based on the kinetics of silver uptake observed, 8 min preconcentration time was chosen for relative silver concentration, as compromise between sufficiently measurable peak current and analysis time.

Table 17 The results of preconcentration time on peak current of 0.5 x 10^{-4} M Ag(I)

Preconcentration time (min)	Current (mA)				
	1st	2nd	3rd	Mean	SD
2.0	0.75	0.83	0.84	0.81	0.049
3.0	1.51	1.49	1.42	1.47	0.047
4.0	2.17	2.18	2.12	2.16	0.032
5.0	3.36	3.34	3.33	3.34	0.015
6.0	4.11	4.07	4.09	4.09	0.020
7.0	5.31	5.32	5.31	5.31	0.015
8.0	6.25	6.26	6.25	6.25	0.015
9.0	6.53	6.55	6.56	6.55	0.025
10.0	6.85	6.89	6.88	6.87	0.021
11.0	7.52	7.54	7.58	7.55	0.031
12.0	7.89	7.92	7.94	7.92	0.025

Table 18 The results of preconcentration time on peak current of 1.0 x 10^{-4} M Ag(I)

Preconcentration time (min)	Current (mA)				
	1st	2nd	3rd	Mean	SD
2.0	2.14	2.15	2.18	2.16	0.021
3.0	4.52	4.48	4.46	4.49	0.031
4.0	5.98	5.95	5.93	5.95	0.025

5.0	6.78	6.83	6.85	6.82	0.036
6.0	7.29	7.32	7.24	7.28	0.040
7.0	8.19	8.23	8.14	8.19	0.045
8.0	8.24	8.25	8.23	8.24	0.010
9.0	8.27	8.31	8.28	8.29	0.021
10.0	8.75	8.74	8.76	8.75	0.010
11.0	8.79	8.71	8.82	8.77	0.057
12.0	9.01	9.07	9.11	9.06	0.050

Table 19 The results of preconcentration time on peak current of 1.5 x 10^{-4} M Ag(I)

Preconcentration time (min)	Current (mA)				
	1st	2nd	3rd	Mean	SD
2.0	4.04	3.98	3.95	3.99	0.046
3.0	6.39	6.42	6.31	6.37	0.057
4.0	7.54	7.50	7.53	7.52	0.021

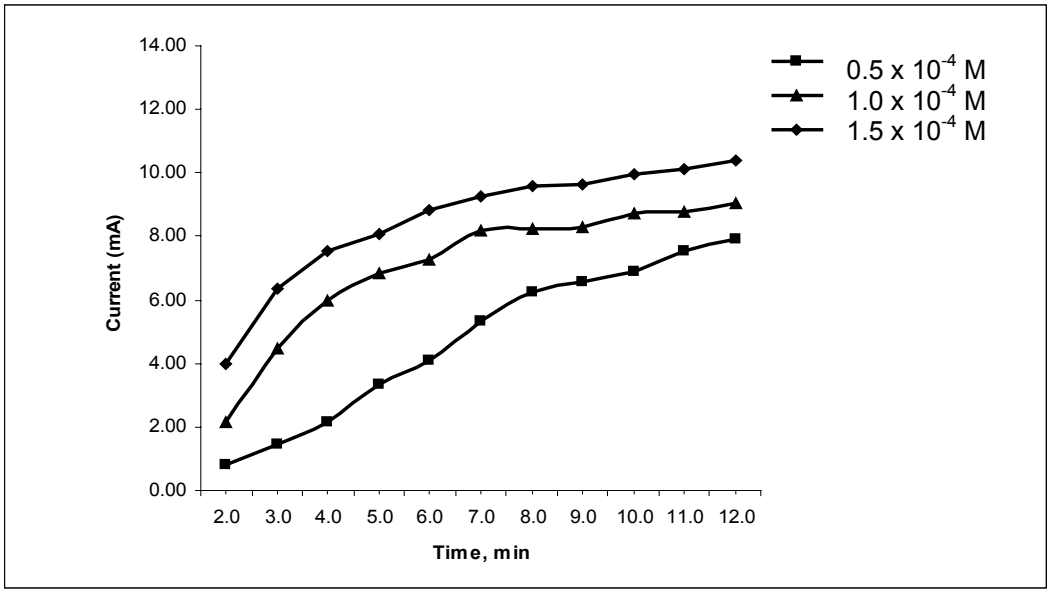

5.0	8.11	8.13	8.07	8.10	0.031
6.0	8.85	8.80	8.78	8.81	0.036
7.0	9.26	9.28	9.22	9.25	0.031
8.0	9.56	9.55	9.57	9.56	0.010
9.0	9.61	9.63	9.69	9.64	0.042
10.0	9.95	9.93	9.97	9.95	0.020
11.0	10.11	10.13	10.09	10.11	0.020
12.0	10.39	10.36	10.38	10.38	0.015

Figure 27 Effect of preconcentration time in CPE -1,8-DHAQ on the stripping peak current of 0.5 x 10^{-4}, 1.0 x 10^{-4} and 1.5 x 10^{-4} M Ag(I). in HNO_3 0.8 M, at -0.20 V with 50 mV of pulse amplitude, 5 mV step potential and 100 Hz of frequency.

3.17.6 Instrumental parameters

3.17.6.1 Accumulation potential

Accumulation potential is an important parameter for stripping techniques and has effect on the sensitivity of determination. It should be sufficiently negative to ensure fast and quantitative reduction of the Ag^{+}-1,8-DHAQ complex on the electrode surface with only a small amount being loss from the surface by diffusion. The effect of the reduction potential on the peak current was investigated in the range of -0.300 to 0.000 V. The peak current appeared starting even from an applied potential of 0.000 V. The result summarized in Table 20-21. The negative shifts of electrode potential can obviously improve the reduction of Ag^{+} on the surface of modified electrode and increase the peak current, as shown in Figure 28. However, the peak current tends to decrease with accumulation potential more negative than -0.250 V due to the fact that at the same time, 1,8-DHAQ may be reduced at these potential (see Figure 11) and interfere the determination of Ag(I). The accumulation potential used in this work is -0.250 V.

Table 20 The currents at various accumulation potentials of 0.5 x 10^{-4} M Ag(I).

Potential	Current (mA)				
(V)	1st	2nd	3rd	Mean	SD
0.00	5.643	5.852	5.714	5.736	0.106
-0.10	5.969	5.885	5.994	5.949	0.057
-0.20	6.237	6.095	6.332	6.221	0.119
-0.25	6.323	6.312	6.298	6.311	0.013
-0.30	6.224	6.101	6.053	6.126	0.088

Table 21 The currents at various accumulation potentials of 1.0 x 10^{-4} M Ag(I).

Potential	Current (mA)				
(V)	1st	2nd	3rd	Mean	SD
0.00	7.251	7.262	7.301	7.271	0.026
-0.10	7.892	7.911	7.921	7.908	0.015
-0.20	8.206	8.215	8.304	8.242	0.054

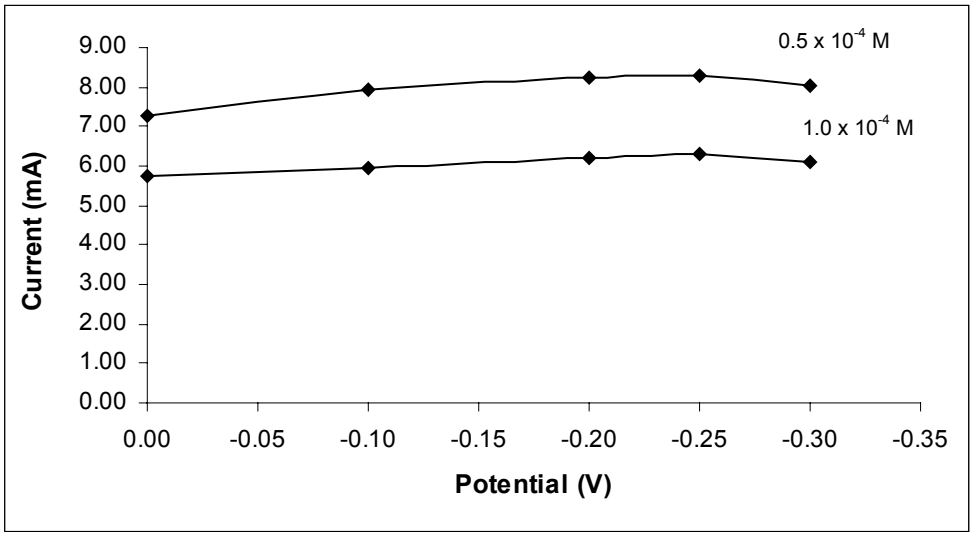

-0.25	8.286	8.405	8.224	8.305	0.092
-0.30	7.987	8.012	8.112	8.037	0.066

Figure 28 Effects of accumulation potentials on stripping current of 0.5 x 10^{-4} and 1.0 x 10^{-4} M Ag(I) with preconcentration time of 8 min with 50 mV of pulse amplitude, 5 mV step potential and 100 Hz of frequency.

3.17.6.2 Convection rate

Migration in the absence of a swamping electrolyte is somewhat more effective than is diffusion, but migration can be ignored if a swamping electrolyte is added to the solution. Diffusion still occurs even if the solution is stirred, but convection is so much more

efficient that the diffusion can ignored completely (Monk, 2001). Mass transport by migration was minimized by adding an electrolyte to electroanalysis solution and convection was wholly eliminated by keeping the solution quiescent. Usually stirring is applied to enhance the rate of the mass transport process. Stirring can be achieved by stirring the solution with the help of a separate stirrer. The standard of Ag(I) of 10 x 10^{-4} M was performed under the optimized working condition describe above. The result summarized in Table 22. The peak current increased with the increasing of convection rate from 1000 to 3000 rpm as in Figure 29. Thus, 3000 rpm was chosen as the convection rate.

Table 22 The response current of 1.0 x 10^{-4} M Ag(I) at different convection rate

Convection rate (rpm)	Current (mA)				
	1st	2nd	3rd	Mean	SD
1000	5.17	5.35	5.28	5.27	0.09
1500	6.96	6.71	6.94	6.87	0.14
2000	7.51	7.56	7.71	7.59	0.10
2500	7.51	7.46	7.62	7.53	0.08
3000	8.52	8.51	8.64	8.56	0.07

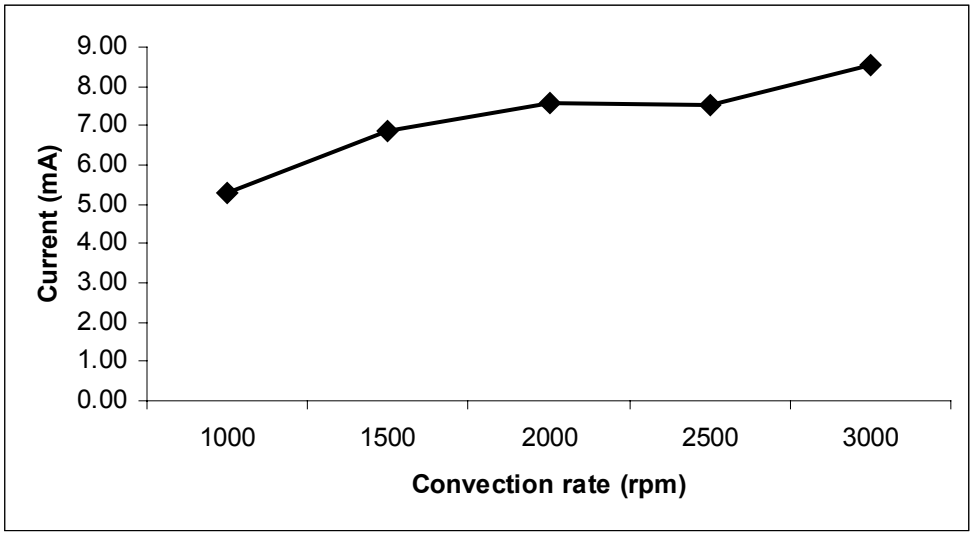

Figure 29 Effect of convection rate on stripping peak of 1.0 x 10^{-4} M Ag(I) with preconcentration time of 8 min at -0.25 V with 50 mV of pulse amplitude, 5 mV step potential and 100 Hz of frequency.

3.17.6.3 Equilibrate time

Equilibrate time is the time for solution quiescent after stirring was stopped. The dependence of the peak current on the equilibrium time was obtained with a solution of Ag^+ of 1.0 x 10^{-4} M. The results are presented in Table 23. As can be ascertained, for equilibration time longer than 10 s an essentially constant response is obtained. On the basis of these results, an equilibration time of 10 s was employed. This was a compromise in term of the speed of the determination and maximum signal. At a solution concentration of silver of 1.0 x 10^{-4} M, the time required for maximum response was 10 s.

3.17.6.4 Effect of step potential and pulse amplitude

To improve the sensitivity for the determination of Ag^+, the influences of parameters of SWASV on the measurement of Ag^+ were studied. The effect of step potential and pulse amplitude on the peak current was studied by varying them in the following range: 0.150-0.090 mV and 25-200 mV respectively. A similar pattern of the peak current was observed upon increasing the individual parameter with constant the frequency as 100 Hz. The results are shown in Table 24-25. The stripping peak current of Ag^+ (1.0 x 10^{-4} M) increases and became broader and broader with increasing the step potential and pulse amplitude and pulse amplitude keeping two of three parameter constant (step potential, pulse amplitude, and frequency) as in Figure 30. Therefore, a step potential of 0.3 mV and pulse amplitude 75 mV were chosen for subsequent experiments. A net current is obtained with difference between the forward and reverse pulse of a square wave period and is plotted versus the potential. Square wave technique coupled with the effective discrimination against the charging background current (Wang, 2000), excellent sensitivity can be obtained.

Table 23 The response current of 1.0 x 10^{-4} M Ag(I) at different equilibrate time

Equilibrate time (s)	Current (mA)				
	1st	2nd	3rd	Mean	SD
0	6.52	7.34	6.97	6.94	0.41
5	7.98	7.73	7.99	7.90	0.15
10	8.46	8.42	8.62	8.50	0.11
15	8.45	8.65	8.31	8.47	0.17
20	8.43	8.63	8.38	8.48	0.13
25	8.52	8.61	8.35	8.49	0.13
30	8.62	8.47	8.35	8.48	0.14

Table 24 The response current of 1.0 x 10^{-4} M Ag(I) at different step potential

Step potential (mV)	Current (mA)				
	1st	2nd	3rd	Mean	SD
0.15	7.31	7.26	7.52	7.36	0.14
0.30	8.37	8.45	8.59	8.47	0.11
0.45	8.46	8.61	8.75	8.61	0.15
0.60	8.66	8.89	8.81	8.79	0.12
0.75	8.91	8.77	9.12	8.93	0.18
0.90	9.41	9.33	9.19	9.31	0.11

Table 25 The response current of 1.0 x 10^{-4} M Ag(I) at different pulse amplitude

Pulse amplitude (mV)	Current (mA)				
	1st	2nd	3rd	Mean	SD
25	4.15	4.61	4.45	4.40	0.23
50	8.29	8.71	8.53	8.51	0.21
75	11.50	11.25	11.54	11.43	0.16
100	14.10	13.85	14.22	14.06	0.19

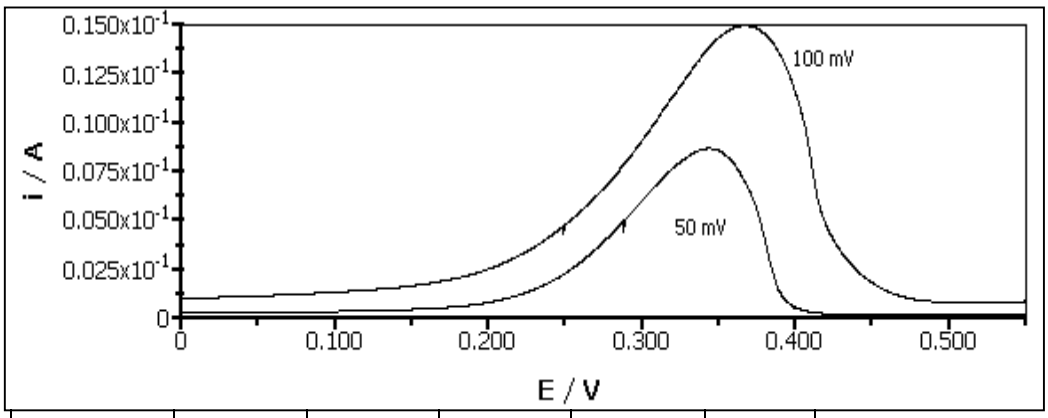

125	17.42	16.59	17.27	17.09	0.44

Figure 30 Stripping voltammogram of 1.0 x 10^{-4} M Ag(I) in 0.8 M HNO_3 (pH 2.00) at CPE-1,8-DHAQ with 8 min preconcentration, -0.25 mV accumulation potential, pulse amplitude 50 and 100 mV, step potential 0.3 mV and 100 Hz frequency.

3.17.7 Regeneration of the working electrode

The extent of electrode regeneration depended on the size of the peak responses, which was related to the amount of accumulated species from the previous run. To utilize the electrode for multiple and long-term operation, the regeneration of the reactive functional groups on the electrode surface in reproducible manner is very important. Different chemical and electrochemical cleaning techniques were tested to restore the electrode surface to its preaccumulation state after each square wave voltammetric determination. The regeneration of the electrode was performed after recorded stripping peak. The efficiency of the cleaning

solutions decreased in order as HNO_3, $NaNO_3$, CH_3COONa, HCl and ultrapure water respectively, as in Table 26. The regeneration of the electrode was performed in the square wave mode with the potential applying at +0.600 V for 2 min under stirred. Electrochemical cleaning at +0.600 V with 0.2 M HNO_3 was successful in renewing the electrode surface. The subsequent voltammetric run gives no peak within potential range indicating that complete removal of any silver remaining the surface.

Table 26 The response current of 1.0 x 10^{-4} M Ag(I) at different chemical regeneration

Condition	Current (mA)								Ip loss (%)[a]
	Before regeneration				After regeneration				
	1st	2nd	3rd	Mean	1st	2nd	3rd	Mean	
$NaNO_3$ 0.1 M	10.7	12.6	11.4	10.8	0.18	0.22	0.19	0.15	98.64
HNO_3 0.2 M	11.6	10.7	11.5	11.3	0.02	0.03	0.04	0.03	99.73
HCl 0.1 M	11.5	10.6	12.2	11.4	1.19	0.25	0.24	0.18	98.45
CH_3COONa	10.9	11.1	11.5	11.2	0.35	0.29	0.37	0.27	97.58
Ultrapure water	11.1	11.9	10.8	11.3	1.25	2.08	2.14	0.30	97.34

[a] Ip loss (%) = [Ip(before)-Ip(after)] x 100/Ip(before)

3.17.8 Reproducibility

The 1,8-DHAQ modified electrode has good reproducibility for the silver ion detection at a single and various electrode surfaces. The results are shown in Table 27. For example, for a single electrode surface the %R.S.D. for the detection of 0.5 x 10^{-4} M Ag^+ after 8 min of preconcentration (number of sample = 8) was 2.30 %. For five electrode surfaces after surface renewal and activation (by performing 8 cycles of

preconcentration/stripping/regeneration), although the stripping step is performed in pH 2, the reproducible data can be obtained because the pH re-equilibrium occurs fast enough. The effective cleaning and reproducible preconcentration were illustrated precision obtained during determination of 0.5 x 10^{-4} M Ag(I). The relative standard deviations were found to be less than 5.00% for eight successive determinations. Slight variations in the peak current (about 5%) were observed for different batches of the electrode containing the same amount of 1,8-DHAQ modified electrode. The preparation of new surface is recommended when eight time of a surface is used.

Table 27 The current response of 1.0 x 10^{-4} M Ag(I) at five new electrode surface

Surface	Current (mA)								Mean	SD	RSD
	1st	2nd	3rd	4th	5th	6th	7th	8th			
1	8.76	8.35	8.94	8.89	8.56	8.63	8.97	8.48	8.70	0.23	2.63
2	8.29	8.95	8.46	8.18	8.93	8.76	8.59	8.86	8.63	0.30	3.42
3	8.16	8.52	9.14	8.67	8.58	9.05	8.47	8.84	8.68	0.32	3.71
4	8.18	8.62	9.06	8.92	9.11	8.55	7.89	8.69	8.63	0.42	4.92
5	8.76	8.95	9.02	8.93	8.26	8.47	8.78	8.97	8.77	0.27	3.08

3.17.9 Calibration graph and linear range

The square wave anodic stripping voltammetric determination of a series of a standard solution of Ag^{+} was performed under the optimized working conditions described above. The results are summarized in Table 28. The calibration graphs as shown in Figure 31 were established by plotting peak height versus various Ag(I) concentration. The result shows that stripping peak current has a linear relationship with concentration in the range of 9.0 x 10^{-6} to 9.0 x 10^{-4} M. The linear correlation coefficient is 0.9942.

Table 28 The current response in different concentration of Ag(I)

Concentration (M)	Current (A)			Mean	SD
	1st	2nd	3rd		
3.0×10^{-6}	2.11×10^{-7}	2.23×10^{-7}	1.18×10^{-7}	1.84×10^{-7}	5.75×10^{-8}
5.0×10^{-6}	3.11×10^{-7}	3.32×10^{-7}	3.37×10^{-7}	3.27×10^{-7}	1.36×10^{-8}
7.0×10^{-6}	4.21×10^{-6}	4.12×10^{-6}	4.21×10^{-6}	4.18×10^{-6}	5.00×10^{-8}
8.0×10^{-6}	9.56×10^{-5}	9.79×10^{-5}	9.66×10^{-5}	9.67×10^{-5}	1.15×10^{-6}
9.0×10^{-6}	1.14×10^{-4}	1.00×10^{-4}	1.21×10^{-4}	1.12×10^{-4}	1.06×10^{-5}
1.9×10^{-5}	1.19×10^{-3}	1.39×10^{-3}	1.53×10^{-3}	1.37×10^{-3}	1.66×10^{-4}
3.0×10^{-5}	3.81×10^{-3}	3.92×10^{-3}	3.82×10^{-3}	3.85×10^{-3}	5.77×10^{-5}
5.0×10^{-5}	8.33×10^{-3}	8.45×10^{-3}	8.52×10^{-3}	8.43×10^{-3}	9.61×10^{-5}
7.0×10^{-5}	1.15×10^{-2}	1.18×10^{-2}	1.21×10^{-2}	1.18×10^{-2}	3.00×10^{-4}
9.0×10^{-5}	1.38×10^{-2}	1.28×10^{-2}	1.35×10^{-2}	1.34×10^{-2}	5.13×10^{-4}
1.0×10^{-4}	1.55×10^{-2}	1.56×10^{-2}	1.57×10^{-2}	1.56×10^{-2}	1.00×10^{-4}
3.0×10^{-4}	1.97×10^{-2}	1.96×10^{-2}	1.95×10^{-2}	1.96×10^{-2}	1.00×10^{-4}
5.0×10^{-4}	2.15×10^{-2}	2.19×10^{-2}	2.21×10^{-2}	2.18×10^{-2}	3.06×10^{-4}
7.0×10^{-4}	2.58×10^{-2}	2.42×10^{-2}	2.41×10^{-2}	2.47×10^{-2}	9.54×10^{-4}
9.0×10^{-4}	2.72×10^{-2}	2.83×10^{-2}	2.89×10^{-2}	2.81×10^{-2}	8.62×10^{-4}

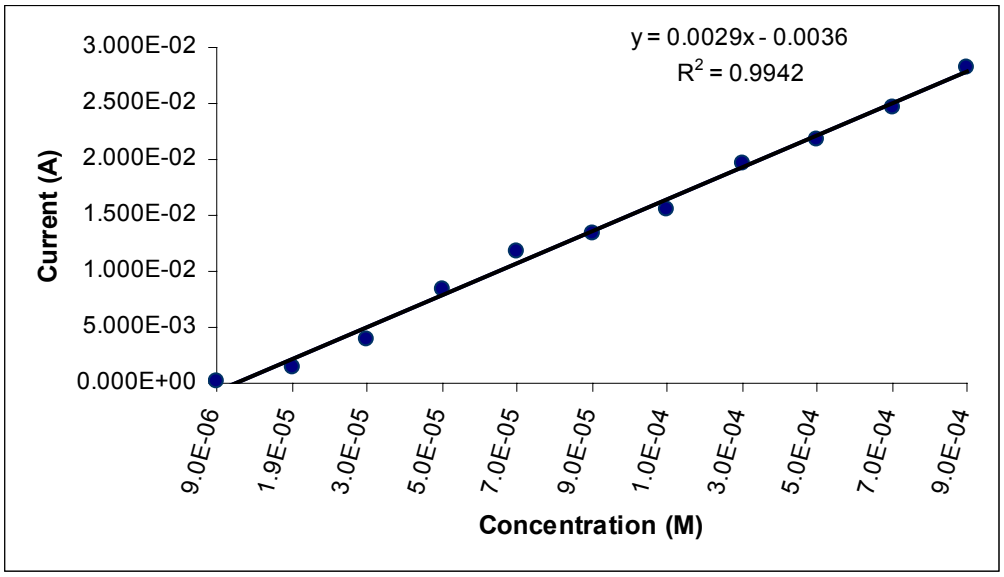

3.17.10 Limit of detection

Limit of detection was considered as the lowest concentration that the CPE modified with 1,8-DHAQ could provide a signal on the voltammogram. Detection limits at 8 min were estimated based on a signal to noise ratio of 3 from the stripping voltammograms. The detection limit improved significantly as the preconcentration time was increased. The detection limit of Ag^{+} at carbon paste electrode modified with 1,8-dihydroxyanthraquinone is 1.39×10^{-7} M.

Figure 31 The Ag(I) calibration curve as current of the peak response after 8 min preconcentration in Ag(I) solutions with varying concentration

3.17.11 Selectivity and interferences

The most significant advantage of carbon paste electrode preconcentration is that the interaction between the 1,8-DHAQ and Ag^{+} at the electrode surface increase the selectivity. Interference can be limited due to the face that any interfering ions must accomplish two necessities. First, the interfering ions can with Ag^{+} for the binding site on 1,8-DHAQ during the preconcentration step. This factor may be indicated by the selectivity of the 1,8-DHAQ for that interfering ions compared with that of Ag^{+}. Second, the interfering ions peak response has a redox potential overlapping Ag^{+} peak in the voltammetric signal. Furthermore, anion form sufficiently stable complexes with Ag^{+} ions can also interfere. The effects of various common

ions were evaluated with respect to their interferences in the determination of Ag(I) by adding 3.0 x 10^{-3} M of foreign ions to 15 mL of solution containing 3.0 x 10^{-5} M Ag^{+} sample solutions during preconcentration. The influence of other ions present in the analyte solution on the current response of Ag(I) is shown in Table 29. Most of the ions studied have only little effect on the determination of Ag^{+}. The results showed that a 100 fold of Cd^{2+}, Co^{2+}, Pb^{2+}, Ni^{2+}, K^{+}, Bi^{3+}, Fe^{3+}, Zn^{2+}, Mg^{2+}, Mn^{2+}, and As^{3+} have only negligible effect on the determination of Ag(I). Because these ions can not effectively complex with 1,8-DHAQ on the surface of modified electrode and the reduction potential of some ions (Zn^{2+}, Pb^{2+}, Cd^{2+}) were present at more negative potential that than of Ag(I). In the presence high concentration of Cu^{2+}, the stripping current of Ag^{+} was interfered significantly by suppressing the Ag^{+} signal due to it can compete with Ag^{+} for complexing at the modified electrode and the stripping peak of Ag^{+} overlaps with Cu^{2+}. The minimum concentration of Cu^{2+} to interfere Ag^{+} analysis was not studied.

Table 29 Change in SWASV peak current of 3.0 x 10^{-5} M Ag(I) in presence of other ions (preconcentration time 8 min)

Interfering ion	added as	Current (mA)				Change in current (%)
		1st	2nd	3rd	Mean	
-	$AgNO_3$	3.81	3.92	3.86	3.86	0.00
Co^{2+}	$Co(NO_3)_2$	3.91	3.85	3.78	3.85	-0.35
Cd^{2+}	$Cd(NO_3)_2$	3.83	3.92	3.86	3.87	0.26
Ni^{2+}	$Ni(NO_3)_2$	3.76	3.86	3.89	3.84	-0.60
Pb^{2+}	$Pb(NO_3)_2$	3.75	3.86	3.94	3.85	-0.26
K^{+}	KNO_3	3.76	3.84	3.87	3.82	-0.95
Bi^{3+}	$Bi(NO_3)_3$	3.65	3.58	3.71	3.65	-5.53
Fe^{3+}	$Fe(NO_3)_3$	3.62	3.68	3.71	3.67	-4.92
Hg^{2+}	$Hg(NO_3)_2$	2.25	2.31	2.34	2.30	-40.41
Zn^{2+}	$Zn(NO_3)_2$	3.85	3.78	3.94	3.86	-0.09
Mg^{2+}	$Mg(NO_3)_2$	3.68	3.59	3.85	3.71	-3.97
Mn^{2+}	$Mn(NO_3)_2$	3.59	3.67	3.85	3.70	-4.06

Cu^{2+}	$Cu(NO_3)_2$	1.96	2.04	1.94	1.98	-48.70
As^{3+}	$As(NO_3)_3$	3.84	3.92	3.87	3.88	0.43
CO_3^{2-}	Na_2CO_3	3.83	3.88	3.73	3.81	-1.21
ClO_4^-	$NaClO_4$	3.68	3.78	3.82	3.76	-2.59
NO_2^-	$NaNO_2$	3.78	3.69	3.86	3.78	-2.16
PO_4^{3-}	Na_2HPO_4	3.87	3.93	3.79	3.86	0.09
NH_4^+	CH_3COONH_4	3.56	3.68	3.76	3.67	-5.01

A 100 fold excess of Hg^{2+} show strong interference due to the face that Hg^{2+} was accumulated on the electrode surface during preconcentration step. Furthermore, oxidation peak of Hg^{2+} overlapped with Ag^+ peak and Hg^{2+} tends to reduced at electrode and form a film on the surface of electrode. The minimum concentration of Hg^{2+} to interfere Ag^+ analysis was not studied. The presence of anions CO_3^{2-}, ClO_4^-, NO_2^- and PO_4^{3-} also did not significantly interfere with the accumulation of Ag(I) onto 1,8-DHAQ. Although some ions interfered in the determination of Ag(I), they did not spoil the electrode surface. On the other hand, some ions influence of weakly interfering ions can easily be eliminated by applying the standard addition method for the evaluation of the concentration of Ag(I). If interfering ions of high concentration exist, CN^- can be added to eliminate the most of interference caused by them (Hu *et al*., 2003). The above results show that the 1,8-DHAQ modified carbon paste electrode has good selectivity for the detection of Ag(I) at the optimum conditions.

3.18 Determination of silver in photographic developer

The analytical procedure described above was used for determination of silver (I) in photographic developer water. The 1:10 diluted water samples showed a distinct peak for silver(I). Hence the concentration of Ag(I) in the water sample is determined by the standard addition method. The Ag(I) standard solution was added with concentration of 1.0×10^{-5} and 2.0×10^{-5} M into sample A and C, respectively which that determined by standard addition method. Three determinations were made on each addition. To certify the reliability of the analytical method, the water samples were also analyzed by ICP-AES. The results obtained with the standard addition method of all sample are given in Table 30-34. Figure 32-36 were plotting

standard addition curve for each diluted sample water which plot mean of peak current (n=3) against silver concentration. The silver concentration of each water samples obtained from the calibration equation is shown in Table 34. Recoveries of 102.00% and 96.05% of Ag(I) were obtained from adding the know amount of Ag(I) into water sample A and C, respectively. This is an evidence of the accuracy of the proposed procedure.

To compare the results obtained from the proposed method and ICP-AES method, the results in Table 35 were from 3 photographic developer water samples. The critical value of *t* is 4.30 at 95% (see APPENDIX B) confidence level with the degree of freedom of 2. It was found that *t* calculated is 0.9945, which is less than *t* critical, therefore, there is no significant difference in results of the CPE-1,8-DHAQ and ICP-AES method.

Table 30 The results of standard addition method of Ag(I) in sample A

Concentration (M)	Current (A)			Mean[a]
	1st	2nd	3rd	
3.00×10^{-5}	5.56410×10^{-3}	5.26450×10^{-3}	5.56370×10^{-3}	$(5.46410 \pm 0.00043) \times 10^{-3}$
5.00×10^{-5}	8.97100×10^{-3}	8.75140×10^{-3}	8.89120×10^{-3}	$(8.87120 \pm 0.00028) \times 10^{-3}$
7.00×10^{-5}	1.48300×10^{-2}	1.47500×10^{-2}	1.49400×10^{-2}	$(1.48400 \pm 0.00024) \times 10^{-2}$
9.00×10^{-5}	1.97900×10^{-2}	1.88080×10^{-2}	2.07990×10^{-2}	$(1.97990 \pm 0.00247) \times 10^{-2}$

[a] mean $\pm$ 95% confidence limits of triplicate analysis

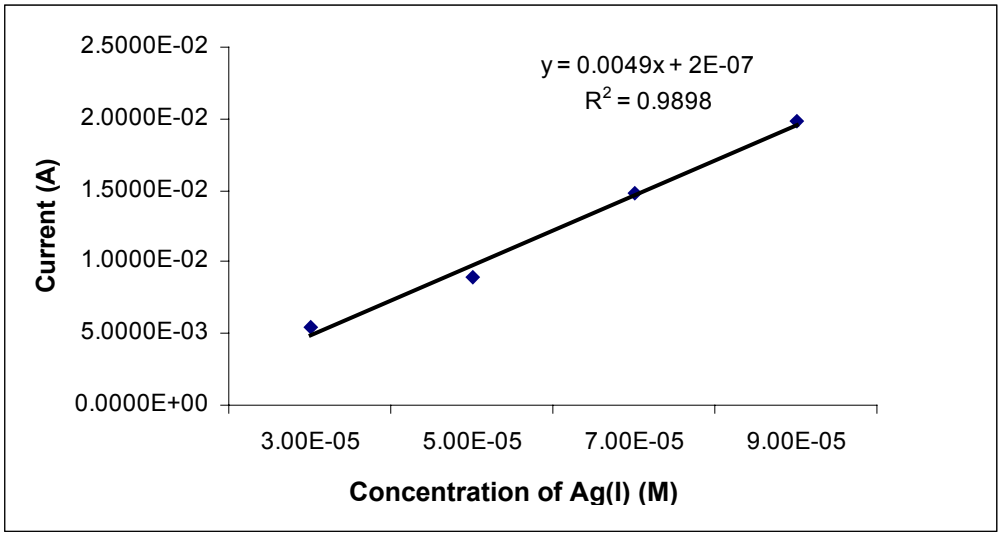

Figure 32 Standard addition curve of Ag(I) in sample A

Table 31 The results of standard addition method of Ag(I) in sample B

Concentration (M)	Current (A)			Mean[a]
	1st	2nd	3rd	
1.00×10^{-5}	5.55500×10^{-3}	5.15000×10^{-3}	5.36000×10^{-3}	$(5.35500 \pm 0.00050) \times 10^{-3}$
3.00×10^{-5}	1.05700×10^{-2}	1.11600×10^{-2}	1.08800×10^{-2}	$(1.08700 \pm 0.00073) \times 10^{-2}$
5.00×10^{-5}	1.68000×10^{-2}	1.59000×10^{-2}	1.78200×10^{-2}	$(1.68400 \pm 0.00238) \times 10^{-2}$
7.00×10^{-5}	2.25770×10^{-2}	2.05790×10^{-2}	2.15810×10^{-2}	$(2.15790 \pm 0.00248) \times 10^{-2}$

[a] mean $\pm$ 95% confidence limits of triplicate analysis

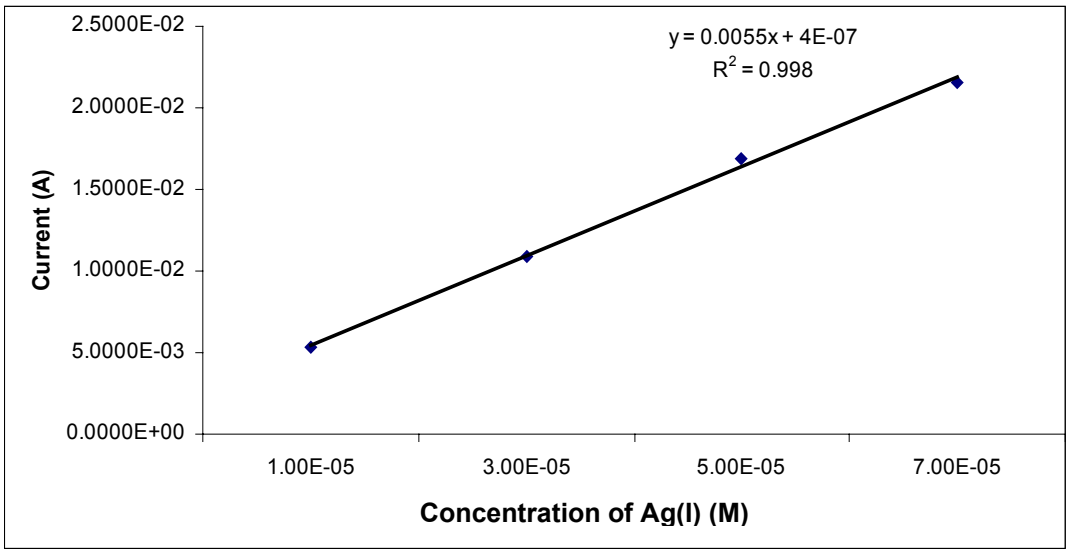

Figure 33 Standard addition curve of Ag(I) in sample B

Table 32 The results of standard addition method of Ag(I) in sample C

Concentration (M)	Current (A)			Mean[a]
	1st	2nd	3rd	
3.00×10^{-5}	4.57620×10^{-3}	4.37651×10^{-3}	4.17690×10^{-3}	$(4.37654 \pm 0.00050) \times 10^{-3}$
5.00×10^{-5}	8.97210×10^{-3}	9.57250×10^{-3}	9.27170×10^{-3}	$(9.27210 \pm 0.00075) \times 10^{-3}$
7.00×10^{-5}	1.29260×10^{-2}	1.31220×10^{-2}	1.27180×10^{-2}	$(1.29220 \pm 0.00050) \times 10^{-2}$
9.00×10^{-5}	1.81250×10^{-2}	1.77300×10^{-2}	1.82200×10^{-2}	$(1.80250 \pm 0.00065) \times 10^{-2}$

[a] mean $\pm$ 95% confidence limits of triplicate analysis

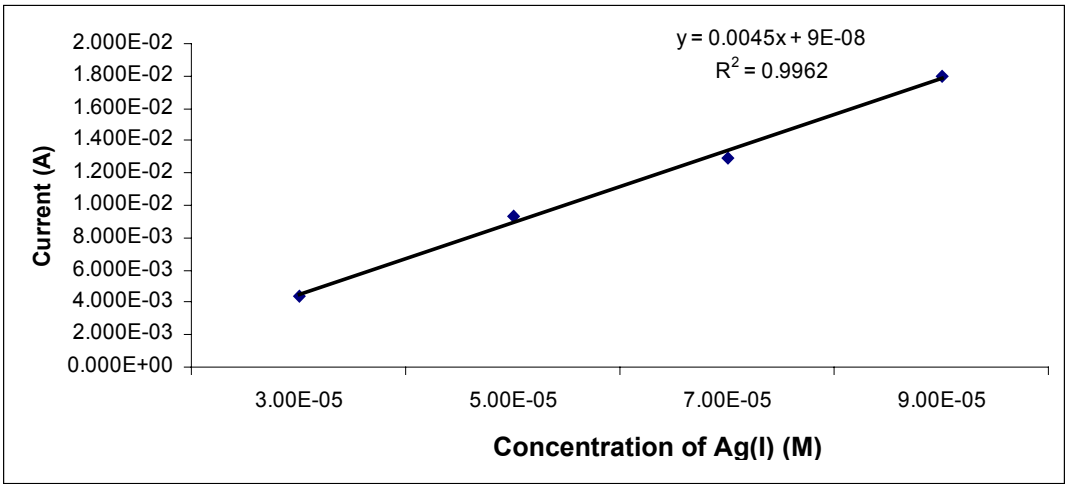

Figure 34 Standard addition curve of Ag(I) in sample C

Table 33 The results of standard addition method of Ag(I) in sample A added 1.0 x 10^{-5} M Ag(I)

Concentration (M)	Current (A)			Mean[a]
	1st	2nd	3rd	
2.00 x 10^{-5}	5.38962 x 10^{-3}	6.48973 x 10^{-3}	6.28960 x 10^{-3}	(6.38965±0.00025)x10^{-3}
4.00 x 10^{-5}	1.14812 x 10^{-2}	1.13822 x 10^{-2}	1.12802 x 10^{-2}	(1.13812±0.00025)x10^{-2}
6.00 x 10^{-5}	1.74400 x 10^{-2}	1.95000 x 10^{-2}	1.53800 x 10^{-2}	(1.74400±0.00511)x10^{-2}
8.00 x 10^{-5}	2.51550 x 10^{-2}	2.31649 x 10^{-2}	2.41598 x 10^{-2}	(2.41599±0.00247)x10^{-2}

[a] mean ± 95% confidence limits of triplicate analysis

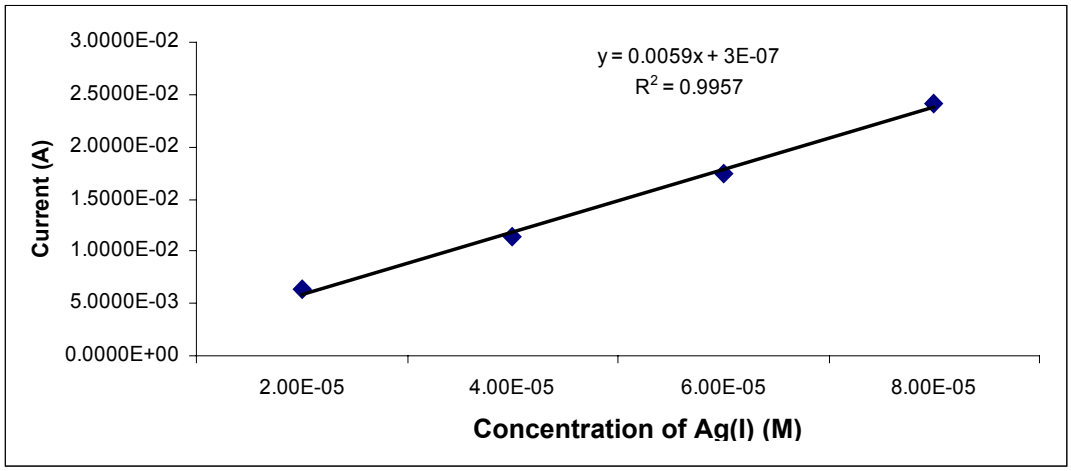

Figure 35 Standard addition curve of Ag(I) in sample A added 1.0 x 10^{-5} M Ag(I)

Table 34 The results of standard addition method of Ag(I) in sample C added 2.0 x 10^{-5} M Ag(I)

Concentration (M)	Current (A)			Mean[a]
	1st	2nd	3rd	
3.00 x 10^{-5}	5.69970 x 10^{-3}	5.60040 x 10^{-3}	5.49900 x 10^{-3}	(5.59970±0.00025)x10^{-3}
5.00 x 10^{-5}	9.07020 x 10^{-3}	8.97215 x 10^{-3}	9.17125 x 10^{-3}	(9.07120±0.00025)x10^{-3}
7.00 x 10^{-5}	1.55200 x 10^{-2}	1.47620 x 10^{-2}	1.66380 x 10^{-2}	(1.56400±0.00234)x10^{-2}
9.00 x 10^{-5}	1.91602 x 10^{-2}	2.03812 x 10^{-2}	2.02702 x 10^{-2}	(2.02700±0.00263)x10^{-2}

[a] mean ± 95% confidence limits of triplicate analysis

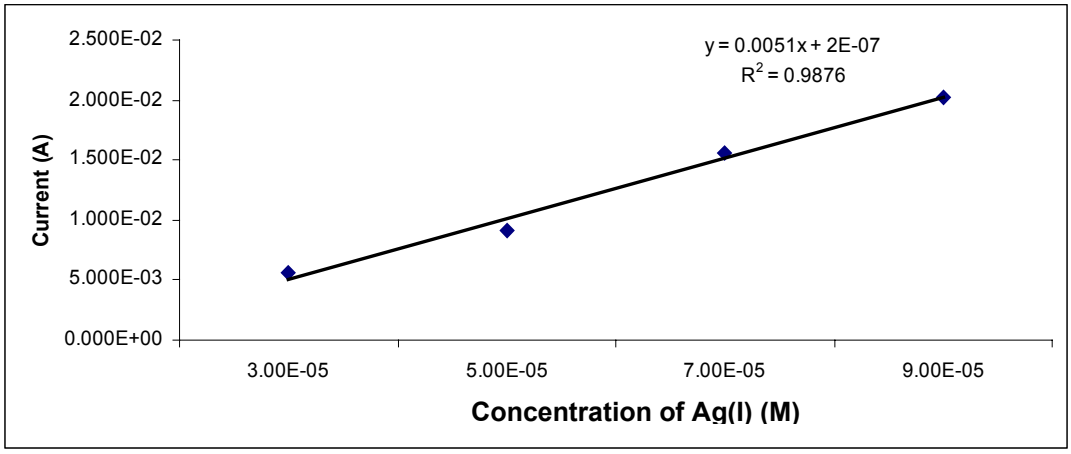

Figure 36 Standard addition curve of Ag(I) in sample C added 2.0 x 10^{-5} M Ag(I)

Table 35 The silver concentrations of samples determined by standard addition method

Sample	Silver added (M)	Silver found x 10 (M) [a]	ICP-AES (M)	Recovery (%)
A	0	4.0811×10^{-4}	4.0582×10^{-4}	not determined
B	0	7.2727×10^{-4}	7.2801×10^{-4}	not determined
C	0	2.0001×10^{-4}	1.9324×10^{-4}	not determined
A	1.0×10^{-5}	5.1010×10^{-4}	not determined	102.0
C	2.0×10^{-5}	3.9210×10^{-4}	not determined	96.05

[a] diluted 10 fold from real sample